AD-A017 395

PRELIMINARY EVALUATION OF THE KOREAN SEISMOLOGICAL RESEARCH STATION SHORT-PERIOD ARRAY

Sidney R. Prahl, et al

Texas Instruments, Incorporated

Prepared for:

Air Force Technical Applications Center
Advanced Research Projects Agency

29 July 1975

DISTRIBUTED BY:

NTIS

National Technical Information Service
U. S. DEPARTMENT OF COMMERCE

APPROVED FOR PUBLIC RELEASE, DISTRIBUTION UNLIMITED

ALEX(01)-TR-75-05

328157

AD A017395

PRELIMINARY EVALUATION OF THE KOREAN SEISMOLOGICAL RESEARCH STATION SHORT-PERIOD ARRAY

TECHNICAL REPORT NO. 5

VELA NETWORK EVALUATION AND AUTOMATIC PROCESSING RESEAHCH

Prepared by
Sidney R. Prahl, Wen-Wu Shen, Richard L. Whitelaw

TEXAS INSTRUMENTS INCORPORATED
Equipment Group
Post Office Box 6015
Dallas, Texas 75222

Prepared for

AIR FORCE TECHNICAL APPLICATIONS CENTER
Alexandria, Virginia 22314

DDC
NOV 19 1975

Sponsored by

ADVANCED RESEARCH PROJECTS AGENCY
Nuclear Monitoring Research Office
ARPA Program Code No. 5F10
ARPA Order No. 2551

29 July 1975

Acknowledgment: This research was supported by the Advanced Research Projects Agency, Nuclear Monitoring Research Office, under Project VELA-UNIFORM, and accomplished under the technical direction of the Air Force Technical Applications Center under Contract No. F08606-75-C-0029.

Reproduced by
NATIONAL TECHNICAL INFORMATION SERVICE
US Department of Commerce
Springfield, VA 22151

UNCLASSIFIED

SECURITY CLASSIFICATION OF THIS PAGE (When Data Entered)

REPORT DOCUMENTATION PAGE		READ INSTRUCTIONS BEFORE COMPLETING FORM
1 REPORT NUMBER	2 GOVT ACCESSION NO.	3 RECIPIENT'S CATALOG NUMBER
4 TITLE (and Subtitle) PRELIMINARY EVALUATION OF THE KOREAN SEISMOLOGICAL RESEARCH STATION SHORT-PERIOD ARRAY		5 TYPE OF REPORT & PERIOD COVERED Technical 6 PERFORMING ORG. REPORT NUMBER ALEX(01)-TR-75-05
7 AUTHOR(s) Sidney R. Prahl, Wen-Wu Shen, and Richard L. Whitelaw		8 CONTRACT OR GRANT NUMBER(s) F08606-75-C-0029
9 PERFORMING ORGANIZATION NAME AND ADDRESS Texas Instruments Incorporated Equipment Group Dallas, Texas 75222		10 PROGRAM ELEMENT, PROJECT, TASK AREA & WORK UNIT NUMBERS VELA T/5705/B/ETR
11 CONTROLLING OFFICE NAME AND ADDRESS Advanced Research Projects Agency Nuclear Monitoring Research Center Arlington, Virginia 22209		12 REPORT DATE 29 July 1975 13 NUMBER OF PAGES 65
14 MONITORING AGENCY NAME & ADDRESS(if different from Controlling Office) Air Force Technical Applications Center VELA Seismological Center Alexandria, Virginia 2231[illegible]		15 SECURITY CLASS (of this report) UNCLASSIFIED 15a DECLASSIFICATION/DOWNGRADING SCHEDULE

16 DISTRIBUTION STATEMENT (of this Report)

APPROVED FOR PUBLIC RELEASE, DISTRIBUTION UNLIMITED

17 DISTRIBUTION STATEMENT (of the abstract entered in Block 20, if different from Report)

18 SUPPLEMENTARY NOTES

ARPA Order No. 2551

19 KEY WORDS (Continue on reverse side if necessary and identify by block number)

Seismology
KSRS Short-Period Array Evaluation
Noise Characteristics
Signal Characteristics
Array Beamforming
Detection Threshold Estimation

20 ABSTRACT (Continue on reverse side if necessary and identify by block number)

A preliminary evaluation of the Korean Seismological Research Station Short-Period Array is presented in this report. Six noise samples from November 1974 were analyzed yielding spectral content, noise amplitudes, multiple coherence, frequency-wavenumber spectra, and noise reduction due to beamforming. Analysis of eight Eurasian teleseismic events from November 1974 included measurements of single-sensor similarity and amplitude variations across the array. In the beamforming studies,

DD FORM 1 JAN 73 1473 EDITION OF 1 NOV 65 IS OBSOLETE

UNCLASSIFIED

SECURITY CLASSIFICATION OF THIS PAGE (When Data Entered)

20. Continued.

time-delay anomalies, spectral content, frequency-wavenumber spectra, signal degradation, signal-to-noise improvements using various beams, and m_b estimates were calculated. A preliminary estimation of the detectability of Eurasian events was also made.

PRELIMINARY EVALUATION OF THE KOREAN SEISMOLOGICAL RESEARCH STATION SHORT-PERIOD ARRAY

TECHNICAL REPORT NO. 5

VELA NETWORK EVALUATION AND AUTOMATIC PROCESSING RESEARCH

Prepared by
Sidney R. Prahl, Wen-Wu Shen, Richard L. Whitelaw

TEXAS INSTRUMENTS INCORPORATED
Equipment Group
Post Office Box 6015
Dallas, Texas 75222

Prepared for

AIR FORCE TECHNICAL APPLICATIONS CENTER
Alexandria, Virginia 22314

Sponsored by

ADVANCED RESEARCH PROJECTS AGENCY
Nuclear Monitoring Research Office
ARPA Program Code No. 5F10
ARPA Order No. 2551

29 July 1975

Acknowledgment: This research was supported by the Advanced Research Projects Agency, Nuclear Monitoring Research Office, under Project VELA-UNIFORM, and accomplished under the technical direction of the Air Force Technical Applications Center under Contract No. F08606-75-C-0029.

ABSTRACT

A preliminary evaluation of the Korean Seismological Research Station Short-Period Array is presented in this report. Six noise samples from November 1974 were analyzed yielding spectral content, noise amplitudes multiple coherence, frequency-wavenumber spectra, and noise reduction due to beamforming. Analysis of eight Eurasian teleseismic events from November 1974 included measurements of single-sensor signal similarity and amplitude variations across the array. In the beamforming studies, time-delay anomalies, spectral content, frequency-wavenumber spectra, signal degradation, signal-to-noise improvements using various beams, and m_b estimates were calculated. A preliminary estimation of the detectability of Eurasian events was also made.

Neither the Advanced Research Projects Agency nor the Air Force Technical Applications Center will be responsible for information contained herein which has been supplied by other organizations or contractors, and this document is subject to later revision as may be necessary. The views and conclusions presented are those of the authors and should not be interpreted as necessarily representing the official policies, either expressed or implied, of the Advanced Research Projects Agency, the Air Force Technical Applications Center, or the US Government.

ACKNOWLEDGMENT

We wish to thank T. W. Harley, S. S. Lane, and R. Unger for their helpful discussions and critical reading of this paper. We also wish to thank Mrs. C. B. Saunders and Mrs. B. C. Taylor who typed and edited the manuscript.

TABLE OF CONTENTS

LIST OF FIGURES

LIST OF FIGURES
(continued)

LIST OF TABLES

SECTION I
INTRODUCTION

The Korean Seismological Research Station (KSRS) Short-Period (SP) Array was designed and implemented to aid in the detection and discrimination of Eurasian events. This report presents the results of a preliminary evaluation to:

- Determine the array's noise and signal characteristics
- Determine the best processing methods for enhancing the signal-to-noise ratios (SNR) of Eurasian events
- Determine the array's detection capability for Eurasian events.

The KSRS SP array, positioned about 110 kilometers (km) southeast of Seoul, Korea and shown in Figure I-1, consists of 19 short-period vertical seismometers and has an aperture of approximately 9 km. Figure I-2 illustrates the arrangement of the seismometers; seismometer 1 is located at 37^{o} 29' N latitude and 127^{o} 54' E longitude.

The data base, discussed in Section II, was taken from the periods 29 April 1973 to 26 July 1973 (eight-hour recordings every other day) and 1 November 1974 to 30 November 1974 (continuous data).

Noise was sampled once each day during the time of least reported seismic activity. Section III discusses the spectral content, root-mean-squared (RMS) noise amplitudes, multiple coherence, high-resolution frequency-wavenumber (f-k) spectra, and noise reduction (due to beamforming) for six representative samples.

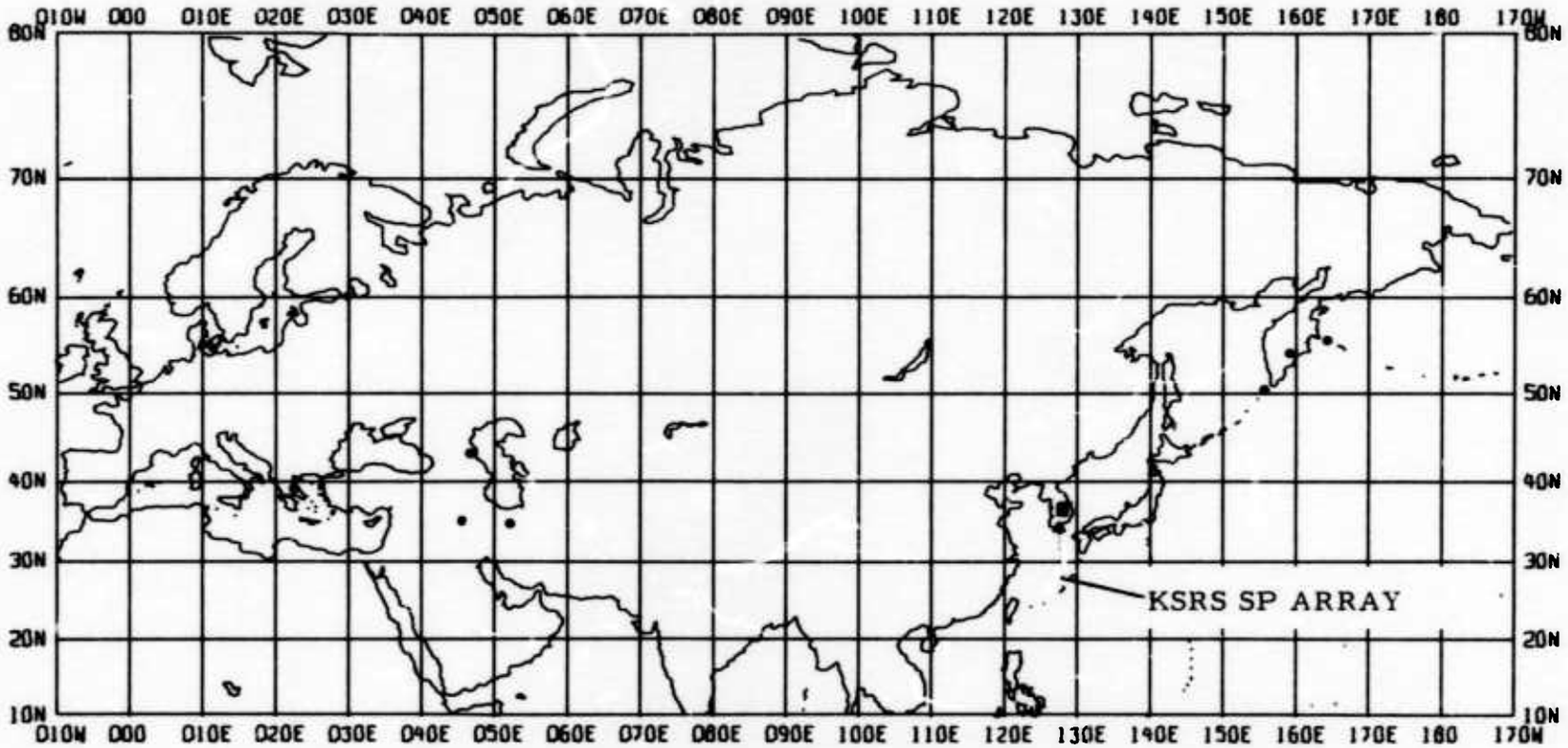

FIGURE I-1

MAP OF EURASIA SHOWING LOCATION OF KSRS ARRAY

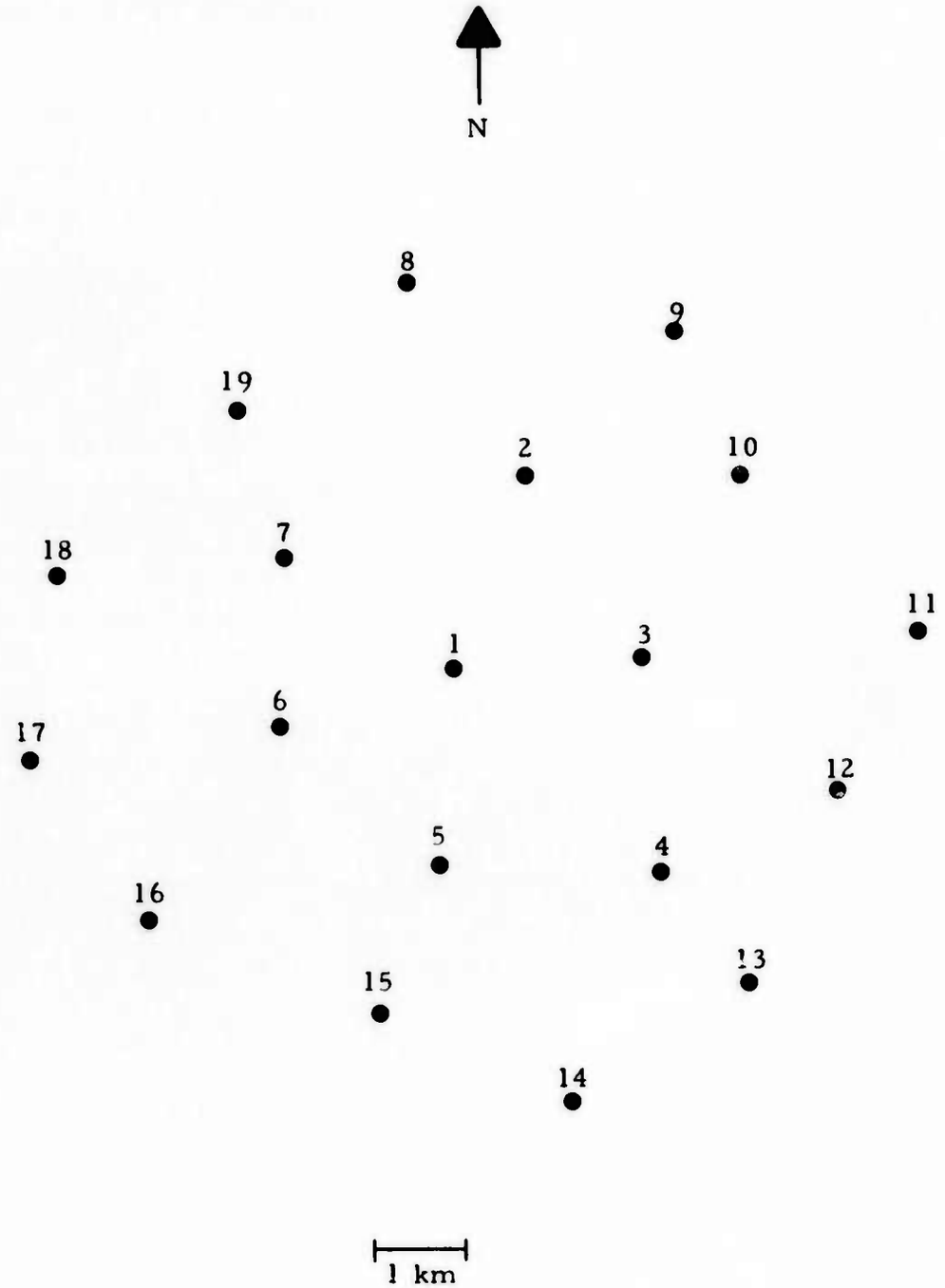

FIGURE I-2

KOREAN SEISMOLOGICAL RESEARCH STATION (KSRS)
SHORT-PERIOD VERTICAL INSTRUMENT LOCATIONS

The combined bulletin lists from NORSAR, LASA, and NOAA yielded 123 Eurasian teleseismic events above $m_b = 3.0$ for the above time periods; KSRS had useable data for 36 of these events. Analysis of eight large events, presented in Section IV, estimated single-sensor signal similarity and amplitude variations. Beamforming results are discussed with regard to time-delay anomalies, spectral content, f-k spectra, signal degradation, SNR improvements using different beams, and KSRS m_b estimates.

A very preliminary estimate of the detectability of Eurasian events is given in Section V, where detection threshold magnitudes were estimated by a maximum likelihood procedure from the detection data for the 36 events.

A summary of results and conclusions are presented in Section VI. References are listed in Section VII.

SECTION II

DATA BASE

Data were available from 29 April 1973 to 26 July 1973 in eight-hour segments taken every other day and during the entire month of November 1974. A search of the NORSAR, LASA, and NOAA bulletins produced 58 Eurasian events from 1973 and 55 from 1974. Twenty-four events could not be edited due to parity and timing errors. Data from only 36 events were useable; the other events were eliminated because of spikes and clipping. All but two events occurred during November 1974.

Table II-1 lists the event parameters. Twenty of the 36 events were detected visually. Ten events had SNR's less than 1.0 dB and eight events had SNR's greater than 5.0. These eight events, five from the Caspian Sea-Greece-Turkey region and three from the Kamchatka region, constitute the samples used in the subsequent signal analyses and are shown in Figure I-1. Each signal sample was 204.8 seconds in duration.

Noise was sampled once each day during the time of least reported seismic activity. Nineteen useable noise samples, of a maximum duration of 640 seconds, were obtained from the November 1974 data. Table II-2 lists the parameters for the noise samples of which six were analyzed in detail.

Data quality of the useable signal and noise samples was very good; on the average 17 sensors were operational at any given time. Sensors 6, 7, 10, 16 and 17 were responsible for the majority of the data losses. Data from the remaining sensors contained few, if any, spikes or clipped peaks.

TABLE II-1

EVENTS ANALYZED

Designation	Date	Origin Time	Lat.	Long.	m_b	Depth	Source	Delta	Comment
GTU/123/01K	05/03/74	01.22.33	38.1N	019.8E	4.0	32	P	79.53	ND
GTU/127/07K	05/07/74	07.41.13	37.1N	029.9E	3.9	33	L	73,79	ND
GTU/306/02K	11/02/74	02.47.12	35.9N	030.2E	3.9	33	L	74.28	ND
SKA/ 306/02K	11/02/74	02.59.51	53.9N	160.4E	4.6	48	P	27.61	SNR< 1.0
CEN/307/10K	11/03/74	10.27.37	44.3N	084.0E	5.4	33	L	33.46	SNR= 2.5
CAS/309/20K	11/05/74	20.02.22	36.2N	052.8E	4.5	68	P	58.39	SNR= 1.4
CAS/310/04K	11/06/74	04.40.57	42.6N	044.3E	4.7	33	L	61.50	SNR< 1.0
SKA/311/15K	11/07/74	15.01.25	50.9N	156.3E	4.4	33	P	24.14	SNR=07.2
NKA/311/20K	11/07/74	20.02.51	55.7N	164.4E	4.7	42	P	30.43	SNR= 9.9
CEN/314/04K	11/10/74	04.31.45	39.3N	073.9E	4.8	33	P	41.72	SNR< 1.0
CEN/314/06K	11/10/74	06.55.51	31.5N	086.4E	4.5	33	P	34.44	SNR< 1.0
NKA/316/03K	11/12/74	03.16.40	52.7N	162.6E	3.9	60	L	28.42	ND
CAS/317/02K	11/13/74	02.36.26	42.7N	046.6E	5.1	42	P	59.93	SNR=10.5
GTU/318/12K	11/14/74	12.41.28	38.6N	023.2E	4.1	12	P	77.15	SNR< 1.0
GTU/318/14K	11/14/74	14.26.46	38.5N	023.0E	5.1	33	P	77.33	SNR=16.0
GTU/318/15K	11/14/74	15.29.45	38.5N	023.1E	5.0	24	P	77.27	SNR=17.5
SKA/318/20K	11/14/74	20.12.45	49.0N	155.8E	4.1	33	L	23.16	SNR< 1.0
GTU/318/22K	11/14/74	22.01.39	40.7N	019.2E	4.0	33	L	78.22	ND
CEN/320/16K	11/16/74	16.18.37	32.8N	076.1E	4.8	63	P	42.08	SNR< 1.0
SIR/321/15K	11/17/74	15.04.48	32.8N	055.1E	5.2	43	P	58.20	ND
CAS/321/15K	11/17/74	15.05.54	33.4N	052.7E	5.7	33	L	59.71	SNR=14.1
SKA/321/17K	11/17/74	17.24.10	54.5N	159.1E	5.0	33	L	27.17	SNR= 5.2
NKA/322/07K	11/18/74	07.16.04	55.3N	161.9E	4.6	33	P	28.96	SNR< 1.0
CAS/322/11K	11/18/74	11.13.30	42.6N	047.1E	3.8	33	L	59.64	ND
NKA/324/05K	11/20/74	05.40.34	54.8N	164.0E	3.6	33	L	29.89	ND
CAS/326/09K	11/22/74	09.05.07	37.6N	048.9E	4.2	33	L	60.57	ND
CAS/327/03K	11/23/74	03.32.36	44.7N	054.1E	4.1	33	L	54.16	ND
GTU/327/09K	11/23/74	09.20.55	39.3N	022.7E	4.0	33	L	77.02	ND
SKA/328/08K	11/24/74	08.31.38	53.7N	159.6E	4.6	33	L	27.10	SNR< 1.0
SKA/328/16K	11/24/74	16.16.35	48.3N	157.1E	4.3	33	L	23.76	ND
SKA/331/11K	11/27/74	11.13.34	52.9N	158.1E	3.9	33	L	25.95	ND
CAS/331/16K	11/27/74	16.52.50	35.3N	045.7E	5.0	50	P	63.92	SNR=17.9
CEN/322/14K	11/28/74	14.57.44	39.5N	075.5E	4.5	33	P	40.47	SNR< 1.0
GTU/333/09K	11/29/74	09.58.40	36.4N	023.1E	4.2	33	L	78.57	ND
SKA/334/05K	11/30/74	05.59.32	47.9N	155.3E	3.7	33	L	22.50	ND
SKA/334/10K	11/30/74	10.30.40	52.9N	158.1E	4.2	33	L	25.95	ND

P = NOAA Bulletin L = SDAC/LASA Bulletin ND = Nondetection SNR = Signal-To-Noise Ratio (dB)

TABLE II-2

NOISE SAMPLES

Designation	Date	Edit Time
NOI/305/05K	11/01/74	05.30.00
NOI/307/07K	11/03/74	07.00.00
NOI/308/08K	11/04/74	08.00.00
NOI/310/10K	11/06/74	10.00.00
NOI/312/12K	11/08/74	12.30.00
NOI/314/21K	11/10/74	21.00.00
NOI/315/17K	11/11/74	17.00.00
NOI/317/09K	11/13/74	09.00.00
NOI/318/09K	11/14/74	09.00.00
NOI/320/14K	11/16/74	14.00.00
NOI/321/16K	11/17/74	16.10.00
NOI/322/10K	11/18/74	10.00.00
NOI/325/06K	11/21/74	06.00.00
NOI/326/13K	11/22/74	13.00.00
NOI/327/06K	11/23/74	06.00.00
NOI/328/15K	11/24/74	15.00.00
NOI/330/20K	11/26/74	20.00.00
NOI/332/11K	11/28/74	11.00.00
NOI/333/14K	11/29/74	14.30.00

The system response for the vertical short-period seismometers is displayed in Figure II-1. The static gain at 1.0 Hertz (Hz) is 0.488 millimicrons (mμ) / count (ct). An anti-aliasing filter eliminated energy above 5.0 Hz. A sampling rate of 20 data points per second (sec) was used for all data.

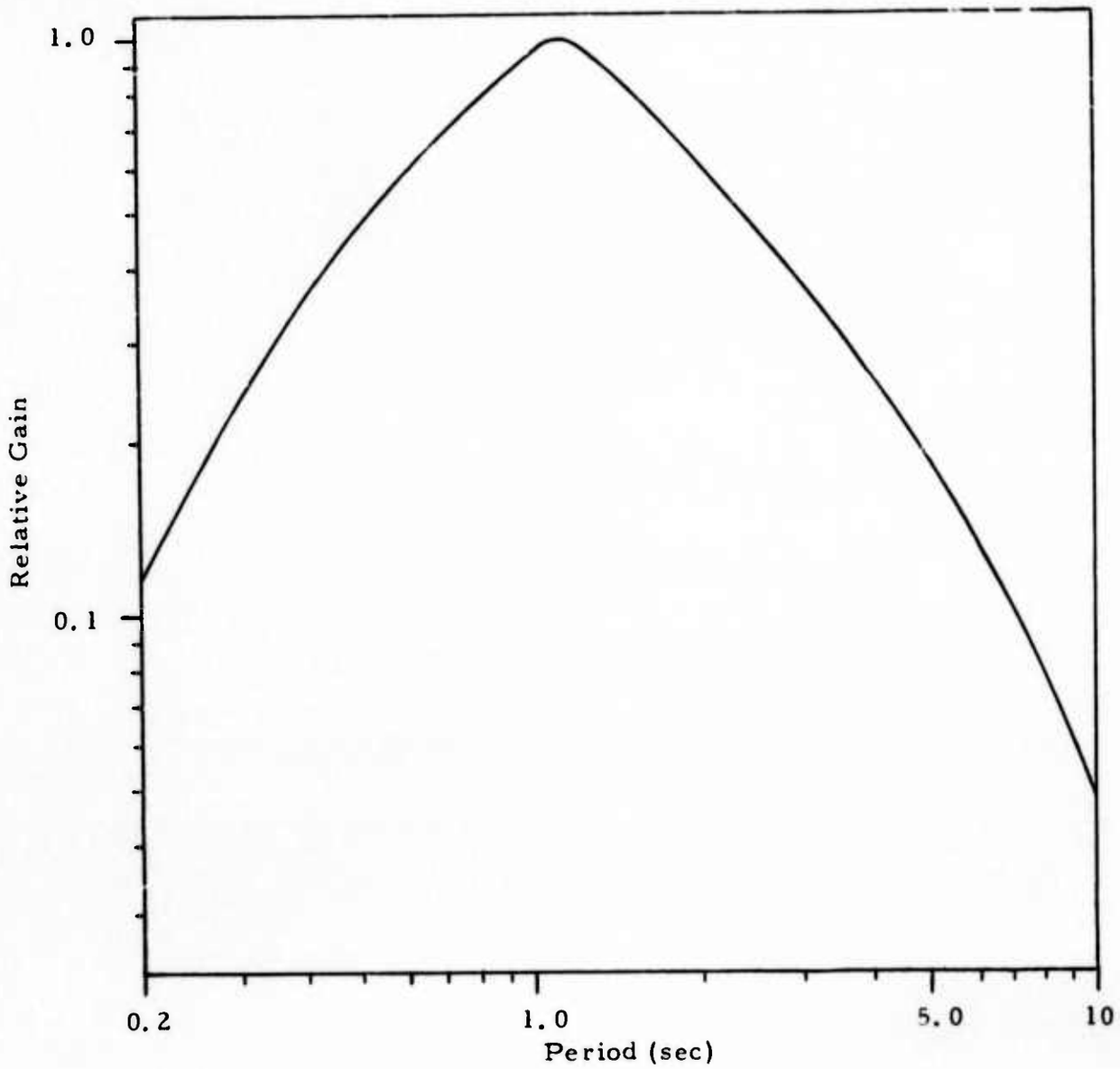

FIGURE II-1

SYSTEM RESPONSE FOR THE KSRS
VERTICAL SP SEISMOMETER

SECTION III
NOISE ANALYSIS

A. INTRODUCTION

This section deals with the KSRS noise field study and is based on six noise samples taken in November 1974: samples NOI/305/05K, NOI/315/17K, NOI/318/09K, NOI/321/16K, NOI/327/06K, and NOI/333/14K. The objective of the study was to characterize the noise field at KSRS to more effectively use signal-enhancement techniques to improve array detection performance. The analysis included the following computations:

- Spectral content
- RMS amplitudes
- Multiple coherence
- High-resolution frequency-wavenumber spectra
- Noise reduction by beamforming.

The data available covered about one month. Accordingly, time variability of the noise was not studied in this report.

B. SPECTRAL CONTENT

Power spectra were computed by averaging at least 80 cross-power spectral matrices from individual contiguous 6.4-second (128 data points) Fourier-transformed segments. The power densities were corrected for instrument response and are relative to 1 $m\mu^2$/Hz.

Figure III-1 presents the instrument-corrected single-sensor power spectrum for sensor 1 averaged over the six noise samples with computed standard deviations at certain frequencies. The maximum power density at 0.16 Hz is in the frequency range where the earth's normal microseismic peak occurs. A second peak at 3.2 Hz, 30 dB lower than the peak at 0.16 Hz, was observed and is discussed in subsection III-E. This peak was not found in the NORSAR spectra (Ringdal and Whitelaw, 1973). Standard deviations of the spectral powers were less than 3 dB except at 0.47 Hz.

Figure III-2 shows the average spectrum across the 19 sensors of the array for sample NOI/315/17K. A maximum variation of about 4.5 dB occurred at 0.16 Hz (which is a true spectral peak as instrument response has been removed from the data). In general, values below 2 Hz had smaller variations than those above 2 Hz, with the exception of values near 0.16 Hz. The 3.2 Hz peak in Figure III-2 is similar to that in Figure III-1.

To summarize, the average noise power spectrum over the six samples and over all sensors is shown in Figure III-3. The noise characteristics are consistent with the presence of high values in the 6-second microseismic band and of a minor peak at 3.2 Hz. The noise power variations across the array were less than 3 dB in the principal band (0.5-3.5 Hz) of interest. Greater variations at higher and lower frequencies were observed.

C. RMS NOISE AMPLITUDES

RMS noise amplitudes were computed for all six samples. Table III-1 gives the results of the computation of averaged single-sensor amplitudes and infinite-velocity beam amplitudes for 204.8 second data segments. Results for both unfiltered and filtered data are presented. In the absence of an optimum filter for the KSRS array, the NORSAR optimum filter (Barnard and Whitelaw, 1972) was used. The standard-filter response is

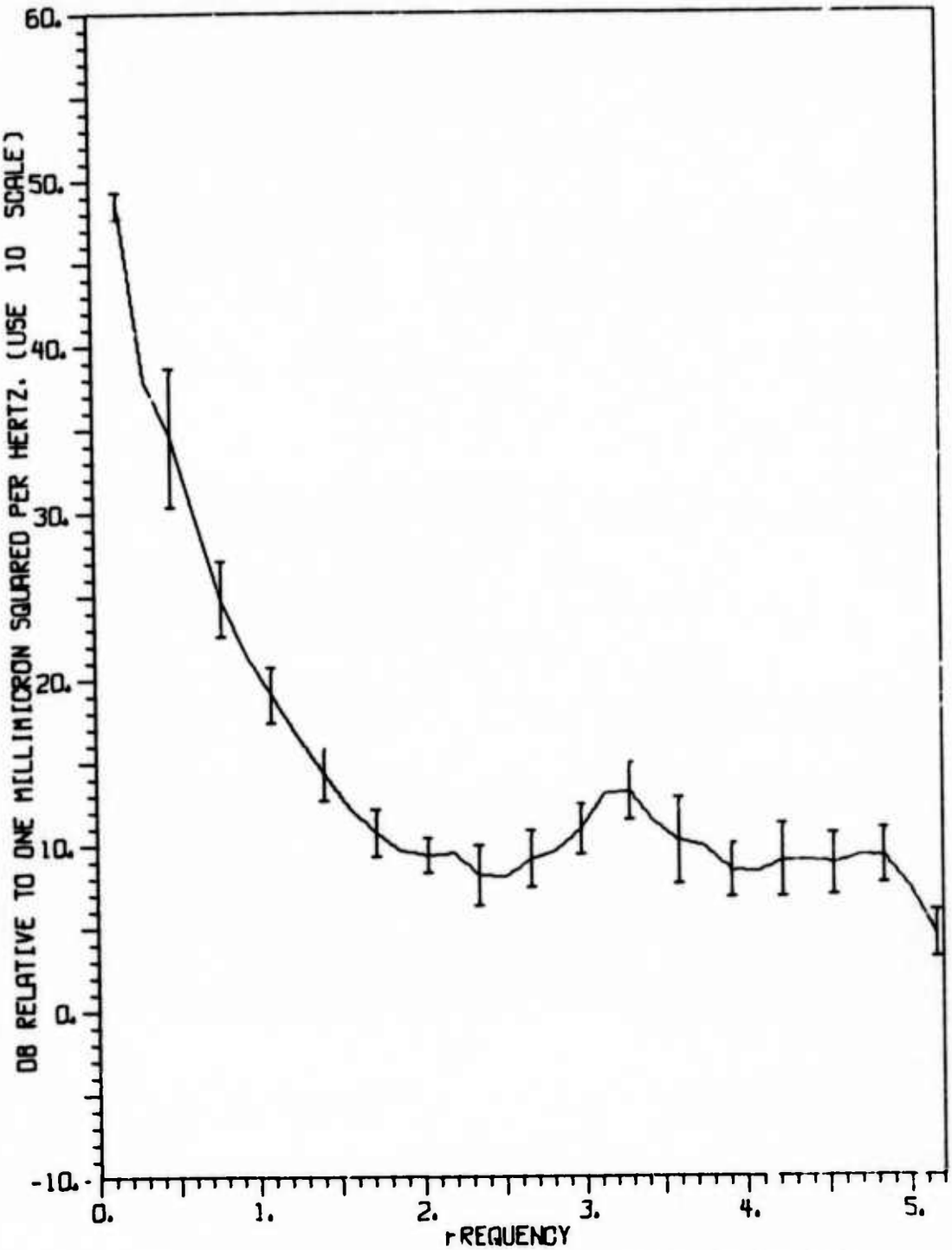

FIGURE III-1

SAMPLE-AVERAGE POWER SPECTRUM FOR SENSOR 1

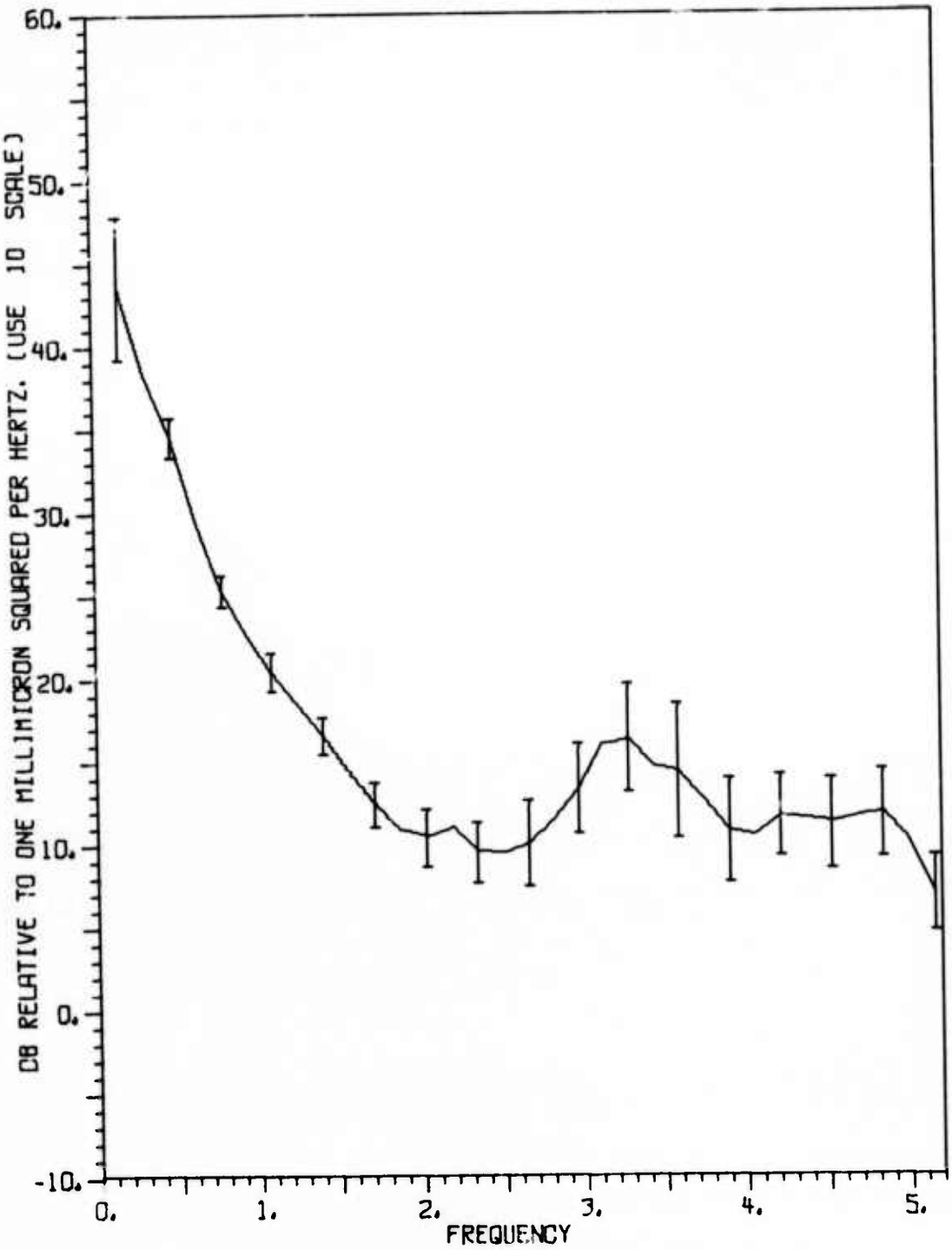

FIGURE III-2

SENSOR-AVERAGE POWER SPECTRUM FOR SAMPLE NOI/315/17K

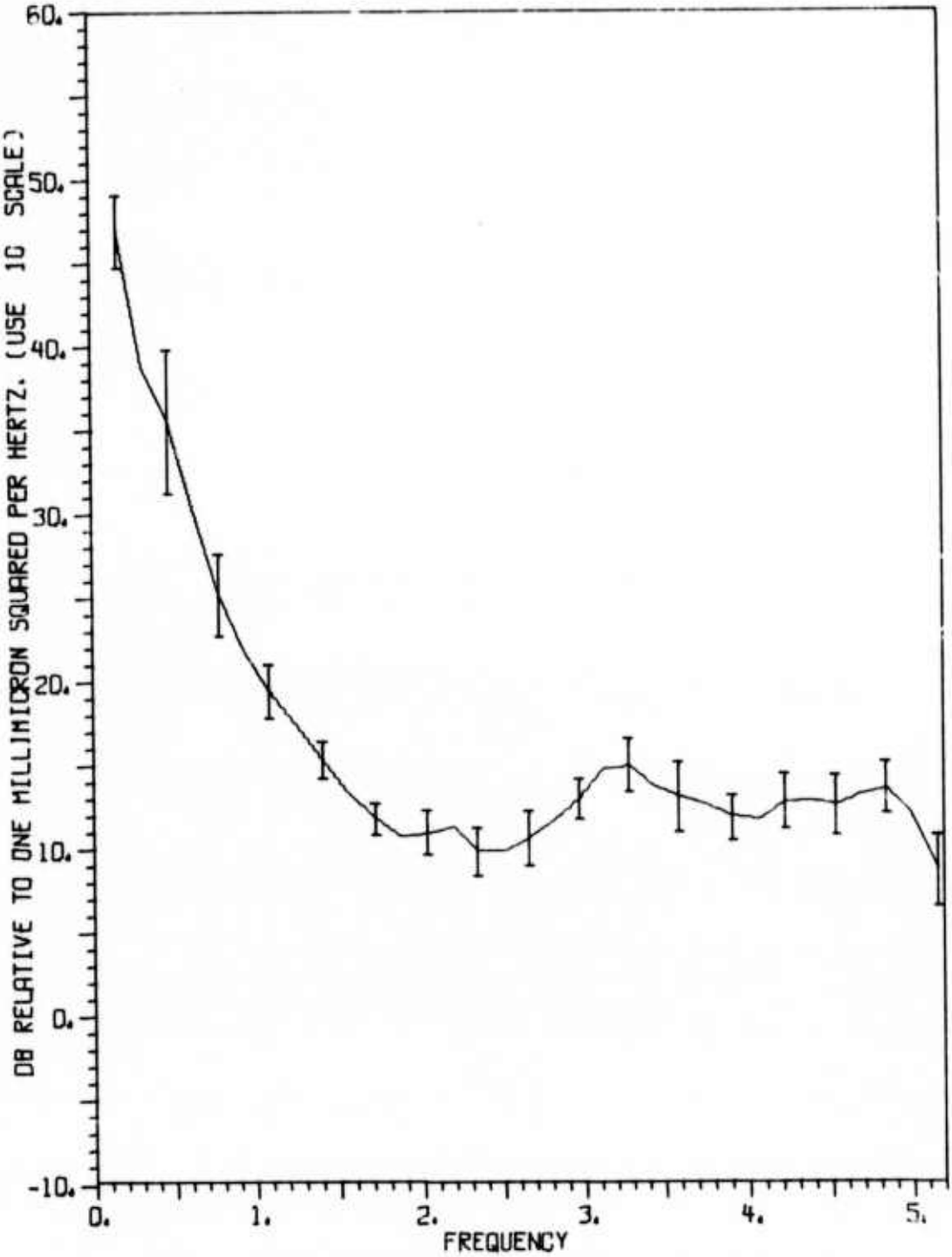

FIGURE III-3

AVERAGE NOISE POWER SPECTRUM FOR NOVEMBER 1974

TABLE III-1

RMS AMPLITUDES FOR SIX NOISE SAMPLES

Noise Sample	Single-Sensor Average		Infinite-Velocity Beam	
	Unfiltered (mμ)	Standard-Filtered (mμ)	Unfiltered (mμ)	Standard-Filtered (mμ)
NOI/305/05K	9.5	1.8	2.1	0.35
NOI/315/17K	9.6	1.8	1.7	0.41
NOI/318/09K	7.1	1.3	1.5	0.31
NOI/321/16K	14.7	1.7	2.7	0.38
NOI/327/06K	18.8	1.7	2.5	0.34
NOI/333/14K	6.0	1.4	1.4	0.31

shown in Figure III-4. All RMS amplitudes were calculated using data uncorrected for instrument response and are relative to 1 Hz; hence, the actual ground-motion RMS amplitudes are higher than those in the table because the dominant noise energy is below 1 Hz.

The RMS amplitudes for single sensors ranged from 6 mμ to approximately 19 mμ for the unfiltered data and from 1.3 mμ to 1.8 mμ for the standard-filtered data. For the infinite-velocity beamformed noise, RMS amplitudes ranged from 1.4 mμ to 2.7 mμ for the unfiltered data and from 0.31 mμ to 0.41 mμ for the standard-filtered data. Beamforming and filtering were seen to have minimized the noise amplitude variations suggesting that the variations were mostly due to the low frequency surface waves around 0.16 Hz. However, similarily calculated RMS noise levels from NORSAR were typically 0.12 mμ, a factor of three lower than the KSRS filtered beam noise levels (Barnard and Whitelaw, 1972).

D. MULTIPLE COHERENCE

Multiple coherence between sensor 1 and the remainder of the array was computed for a number of cases (Texas Instruments, Inc., 1971). Sample results for two cases are presented here. Figure III-5 shows multiple coherence as a function of frequency for sample NOI/315/17K. Curve A was computed by correlating sensor 1 with the rest of the inner ring (sensors 2-7), and curve B by correlating sensor 1 with part of the outer ring (sensors 8-13). The two cases used the same number of sensors in order to make possible a comparison of coherence for different spatial separations.

Coherence was higher for the inner ring with a diameter of 4.5 km, than for the outer ring with a diameter of 9 km. At frequencies higher than 0.5 Hz and for an array diameter of 9 km, the coherence was relatively low; hence, for effective signal enhancement, elimination of low frequency noise energy (less than 0.5 Hz) is essential.

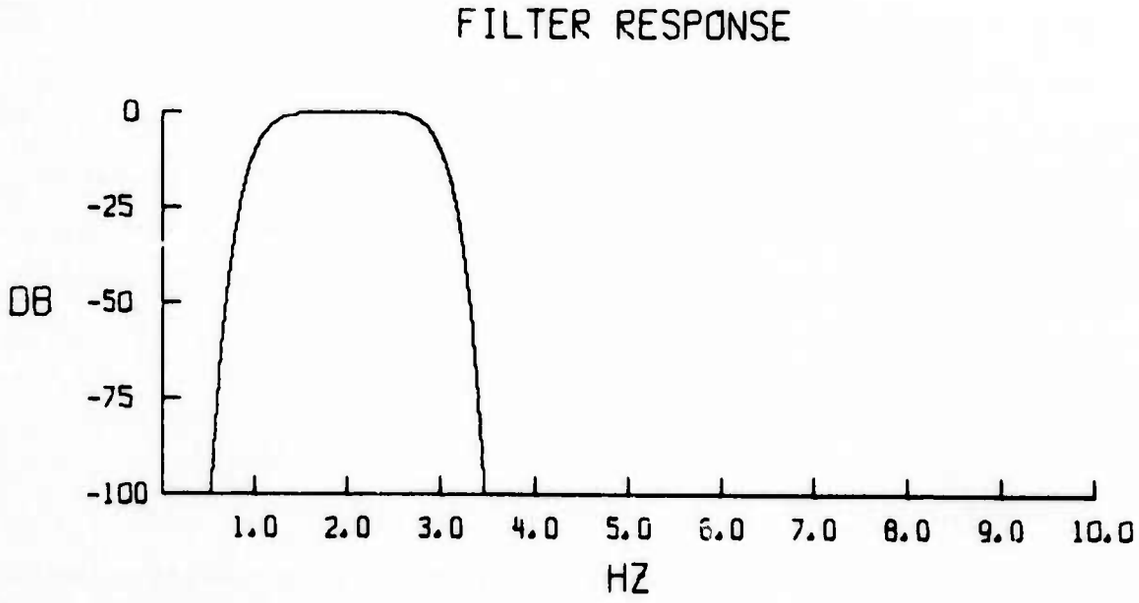

FIGURE III-4

STANDARD-FILTER RESPONSE

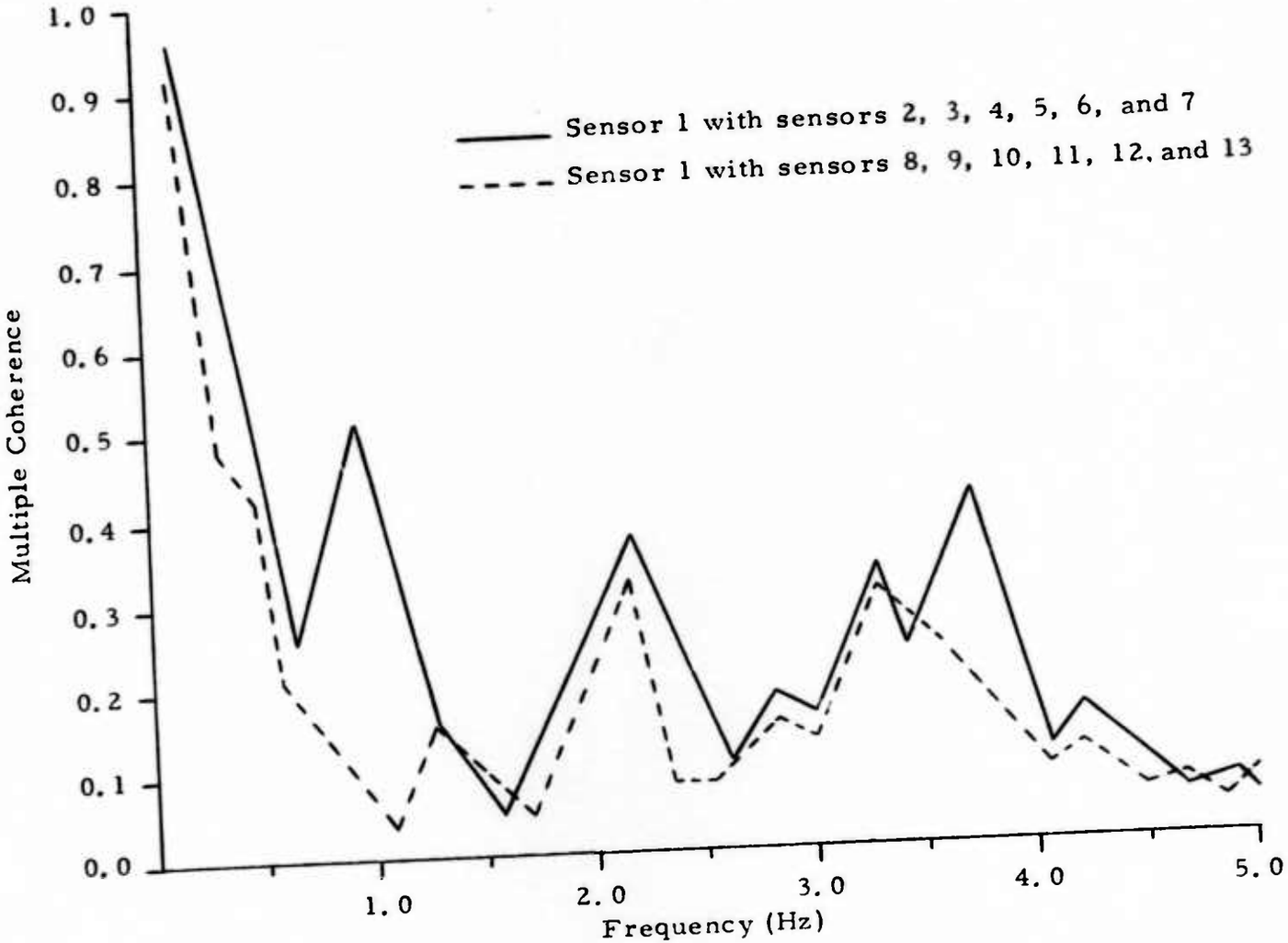

FIGURE III-5

MULTIPLE COHERENCE FOR SAMPLE NOI/315/17K

Figure III-6 shows the results of the same computations for sample NOI/327/06K which had the highest RMS amplitudes. Similarity between the two noise samples is pronounced. Computations of coherence using other sensor geometries gave results similar to these for all samples.

E. FREQUENCY-WAVENUMBER SPECTRA

This subsection describes the analysis of the frequency-wavenumber spectra of the noise samples (Texas Instruments, Inc., 1971). The f-k spectra were computed at 0.31, 0.47, 0.94, and 3.3 Hz. Due to the fact that the diameter of the array (9 km) was less than one wavelength at 0.16 Hz, the spectrum was not significant and, therefore, the microseismic peak energy was not examined by this method.

Figure III-7 illustrates an f-k spectrum at 0.31 Hz for sample NOI/315/17K, where phase velocity ranges from 2 km/sec at the edge to infinity at the center. The figure shows energy propagating from 197^{o} with a 3.4 km/sec velocity, that of Rayleigh waves. The -3 dB contour indicates that the noise source was diffuse. The f-k spectrum also suggests a secondary surface wave source from the northeast, 6 dB lower than the principal source.

Figure III-8 shows an f-k spectrum at 0.47 Hz for the same sample. The principal peak from the southwest and the secondary peak, 5 dB lower than the principal peak, from the northeast are in agreement with those of the 0.31 Hz spectrum. Slight azimuthal variations were probably caused by scattering. The consistency is further demonstrated in Figure III-9 where the f-k spectrum at 0.94 Hz is shown.

The f-k spectrum at 3.3 Hz indicated that the noise causing this spectral peak was random.

Table III-2 summarizes the results of the f-k spectral study for the six noise samples. Results at frequencies up to 0.94 Hz suggest that noise in the low frequency band of 0.31-0.94 Hz is composed of Rayleigh-

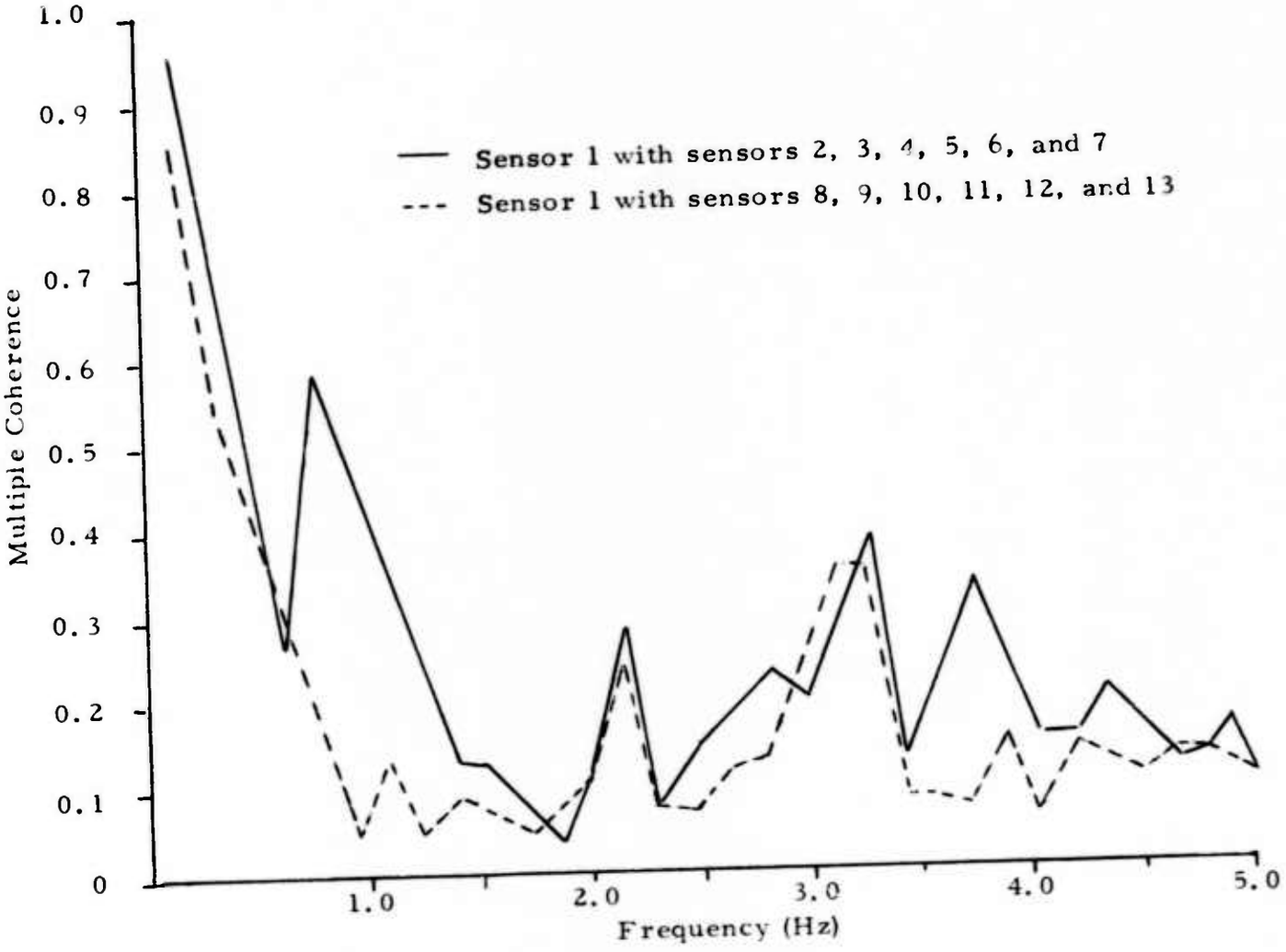

FIGURE III-6

MULTIPLE COHERENCE FOR SAMPLE NOI/327/06K

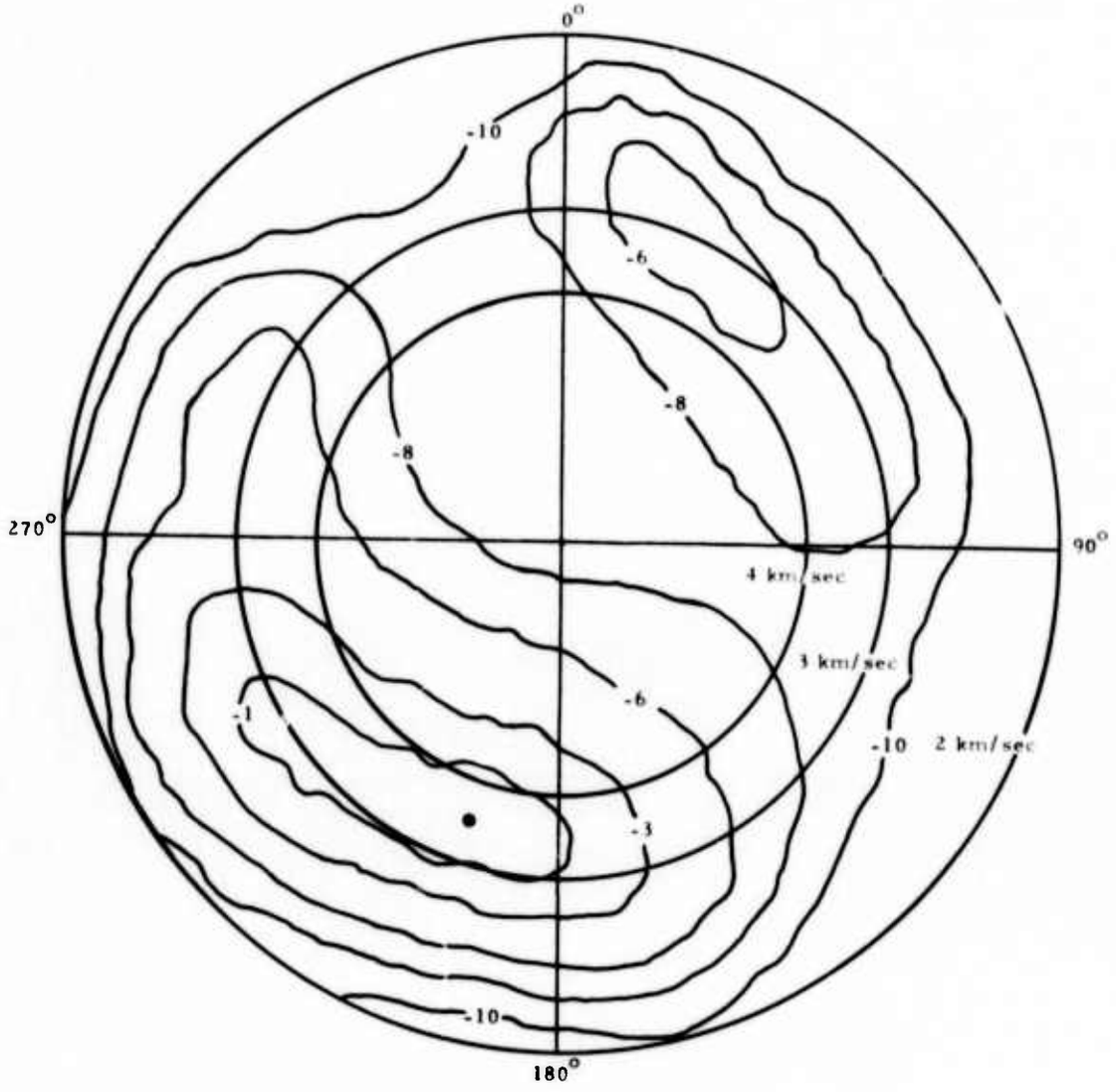

FIGURE III-7

FREQUENCY-WAVENUMBER SPECTRUM AT
0.31 Hz FOR SAMPLE NOI/315/17K

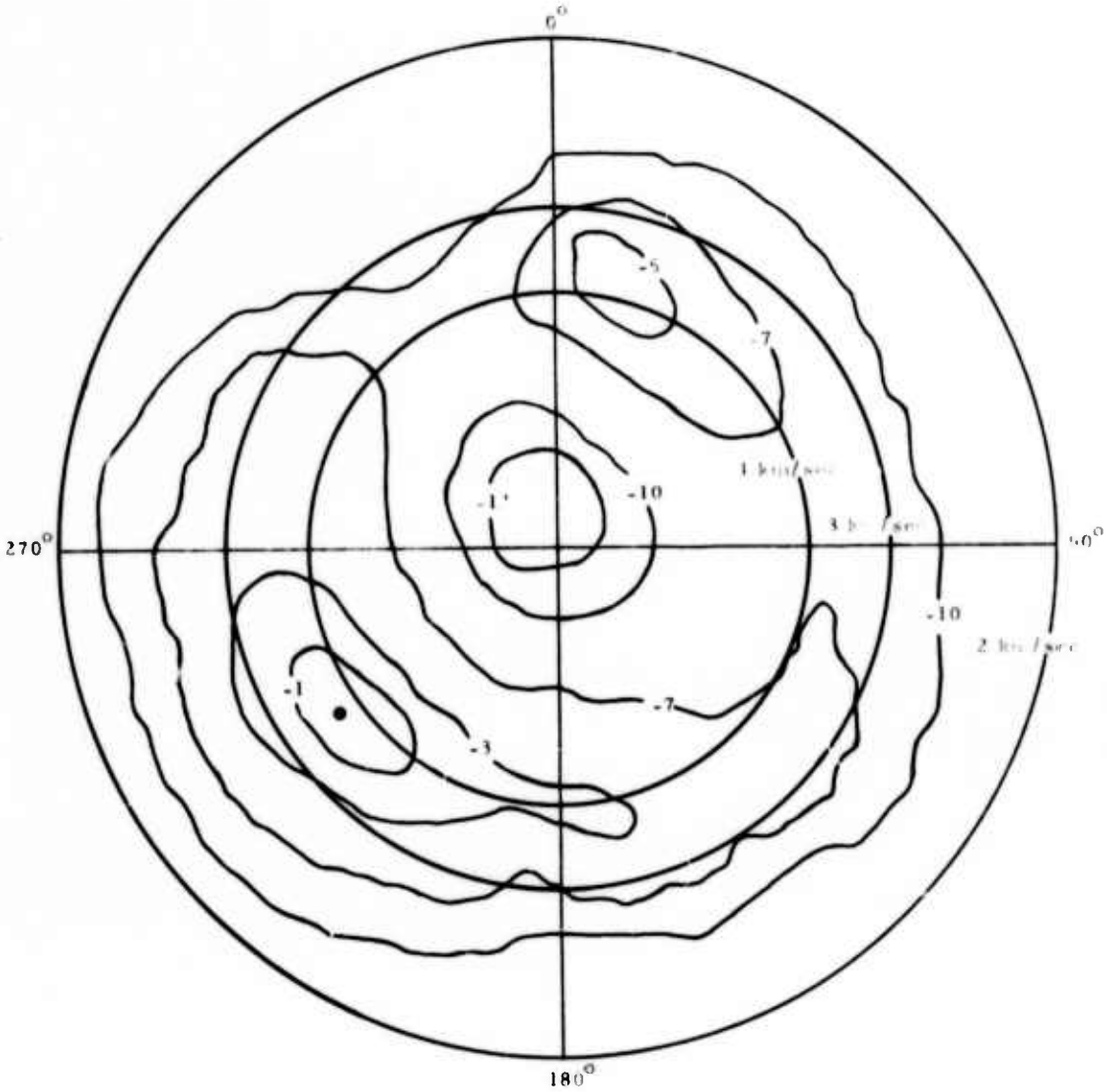

FIGURE III-8

FREQUENCY-WAVENUMBER SPECTRUM AT
0.47 Hz FOR SAMPLE NOI/315/17K

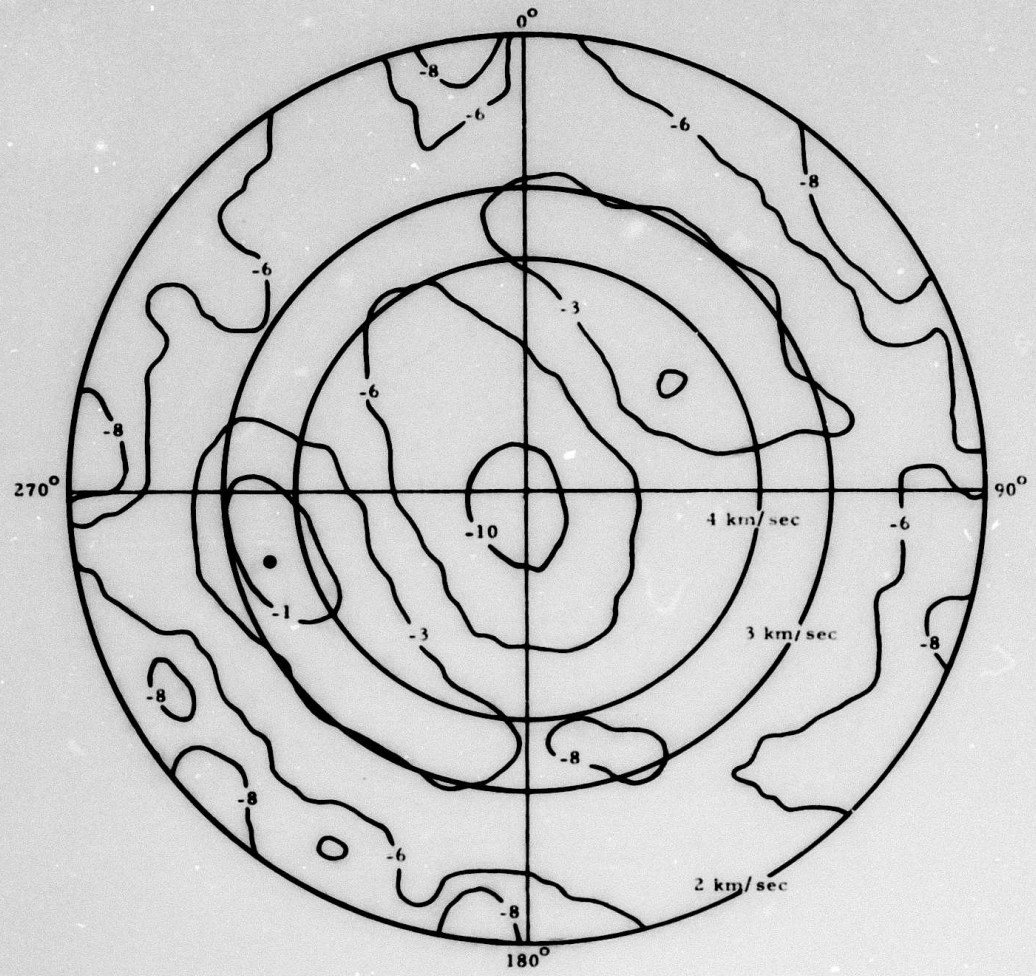

FIGURE III-9

FREQUENCY-WAVENUMBER SPECTRUM AT
0.94 Hz FOR SAMPLE NOI/315/17K

TABLE III-2

SUMMARY OF f-k SPECTRAL ANALYSIS FOR THE SIX NOISE DATA SAMPLES (PAGE 1 OF 3)

Noise Sample	Frequency (Hz)	Peak Azimuth (Degree)	-3 dB Azimuthal Range (Degree)	Velocity (km/sec)	Comments
NOI/305/05K	0.31	237	64-256	2.6	Rayleigh Mode
	0.47	239	192-304	3.4	Rayleigh Mode
	0.94	261	142-115	3.2	-1 dB peaks at 12^{o} and 3.3 km/sec and at 60^{o} and 3.5 km/sec. Rayleigh Mode
	3.30	215	-	13.0	-1 dB peaks at 330^{o} and 8 km/sec, 50^{o} and 17 km/sec and 92^{o} and 10 km/sec.
NOI/315/17K	0.31	197	165-260	3.4	Rayleigh Mode
	0.47	233	168-264	3.5	Rayleigh Mode
	0.94	254	184-284	3.4	Secondary peak (-1 dB) at 55^{o} with 4.8 km/sec. Rayleigh Mode
	3.30	261	-	6.0	-1 dB peaks from various azimuths and velocities.

TABLE III-2

SUMMARY OF f-k SPECTRAL ANALYSIS FOR THE SIX NOISE DATA SAMPLES (PAGE 2 OF 3)

Noise Sample	Frequency (Hz)	Peak Azimuth (Degree)	-3 dB Azimuthal Range (Degree)	Velocity (km/sec)	Comments
NOI/318/09K	0.31	237	184-258	2.7	Rayleigh Mode
	0.47	236	194-258	3.4	Rayleigh Mode
	0.94	71	320-113	3.7	-1 dB peak at 220° and 4 km/sec. Rayleigh Mode
	3.30	90	-	17.0	-1 dB peaks from various azimuths and velocities.
NOI/321/16K	0.31	245	200-265	3.0	Rayleigh Mode
	0.47	247	207-279	3.0	Rayleigh Mode
	0.94	240	201-280	3.8	Rayleigh Mode
	3.30	99	-	9.0	-1 dB peaks from various azimuths and velocities.

TABLE III-2

SUMMARY OF f-k SPECTRAL ANALYSIS FOR THE SIX NOISE DATA SAMPLES
(PAGE 3 OF 3)

Noise Sample	Frequency (Hz)	Peak Azimuth (Degree)	-3 dB Azimuthal Range (Degree)	Velocity (km/sec)	Comments
NOI/327/06K	0.31	250	222-282	2.6	Rayleigh Mode
	0.47	246	222-282	3.6	Rayleigh Mode
	0.94	81	42-112	4.3	-1 dB peak at 230^{o} and km/sec. Rayleigh Mode
	3.30	257	-	6.0	-1 dB peaks at various azimuths and velocities. Random noise.
NOI/333/14K	0.31	197	158-246	3.3	Rayleigh Mode
	0.47	237	9-271	3.3	-1 dB peaks at 165^{o} and 3.3 km/sec and at 80^{o} and 3.6 km/sec. Rayleigh Mode
	0.94	72	12-116	4.2	-1 dB peak at 255^{o} and 3.3 km/sec. Rayleigh Mode
	3.30	32	-	15.0	-1 dB peaks at various azimuths and velocities. Random noise

mode surface waves propagating from the southwest and northeast. Clear separations of wavenumber peaks with a common azimuth such as found at LASA (Haubrich and McCamy, 1969) were not seen in the spectra. Consequently, identification of Rayleigh-wave fundamental and higher modes was not possible. Energy at the 3.3 Hz peak (which is 25-30 dB below the 6-second peak) appeared to be random.

F. NOISE REDUCTION

Figure III-10 shows the average sensor and the infinite-velocity beam power spectra computed from sample NOI/315/17K for 17 sensors. Noise reduction achieved by beamforming is shown by the solid line and generally is higher than 10 log (number of sensors), the theoretical random noise reduction shown by the horizontal line at 12.3 dB. The KSRS array response for an infinite-velocity beam showed 19 dB rejection at 0.47 Hz and 26 dB rejection at 0.64 Hz for 3.6 km/sec Rayleigh-mode energy. The increased noise suppression found here is, therefore, consistent with the presence of propagating surface-wave energy found in subsection III-E.

Table III-3 shows average sensor to infinite-velocity beam RMS power ratios for the six noise samples. Both unfiltered and standard-filtered results are shown along with the theoretical noise reduction. The suppression was generally higher for unfiltered data than for the standard-filtered data due to the greater suppression of Rayleigh-mode noise in the frequency band from 0.0 to 0.5 Hz. The standard-filter noise reduction was close to 10 log (number of sensors) implying the dominance of random noise above 1 Hz. Similar results were obtained for a north-looking beam at 15 km/sec which corresponds to an epicentral distance of 50 degrees.

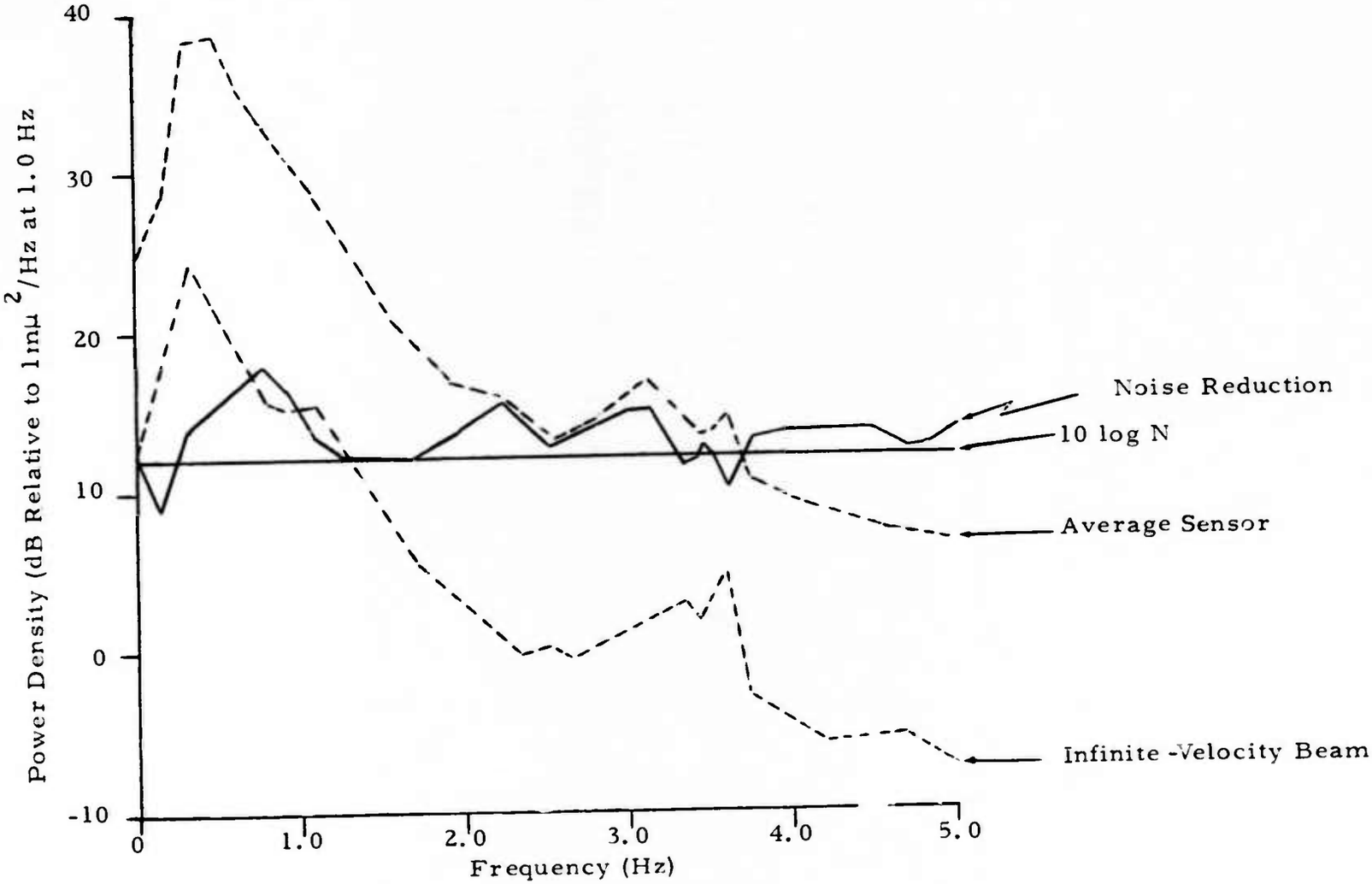

FIGURE III-10

AVERAGE SENSOR AND INFINITE-VELOCITY BEAM POWER SPECTRA AND RESULTANT NOISE REDUCTION FOR SAMPLE NOI/315/17K

TABLE III-3

NOISE REDUCTION DUE TO BEAMFORMING

Noise Samples	Number of Sensors (N)	Noise Reduction (dB)		
		Unfiltered	Standard-Filtered	10 log N
NOI/305/05K	18	13.1	14.1	12.5
NOI/315/07K	17	15.1	12.7	12.3
NOI/318/09K	17	13.7	12.5	12.3
NOI/321/16K	17	14.6	12.8	12.3
NOI/327/06K	19	17.2	13.8	12.8
NOI/333/14K	17	12.9	12.8	12.3

G. CONCLUSIONS

Six KSRS noise samples, covering November 1974, had high spectral values in the 6 second microseismic band and a minor peak at 3.2 Hz. The spectral shapes were very similar to those at NORSAR except at 3.2 Hz. No significant temporal or spatial variations in the noise spectra were observed in the band of interest. The single-sensor RMS noise amplitudes had modal values of 5-7 mμ. Multiple coherence computations and filtered RMS noise amplitudes suggest that energy in the band below 0.5 Hz was correlated and should be eliminated for best beamforming results. The f-k spectral analysis indicates that the noise below 1 Hz was caused by Rayleigh-mode surface waves from the southeast while the noise above 1 Hz was random. The average noise reduction due to beamforming was 13.1 dB.

SECTION IV
SIGNAL ANALYSIS

A. INTRODUCTION

Eight events recorded by the KSRS array were analyzed to study signal characteristics. The analysis included the following calculations:

- Signal similarity among sensors
- Single-sensor amplitude variations
- Time-delay anomalies
- Spectral content
- f-k spectra
- Signal degradation
- SNR improvements using different beamforming methods
- Comparison of KSRS magnitudes (m_b) with NOAA and LASA magnitudes.

A detailed description of plane-wave, adjusted-delay, and diversity-stack beams can be found in the Documentation of NORSAR Short Period Array Evaluation Software Package (Texas Instruments, Inc., 1971); however, a brief description of these beams is given here.

The plane-wave beam represents the normalized sum of the traces from all sensors after time shifting according to the sensor's geometric location in the array. The adjusted-delay beam uses time shifts computed by crosscorrelating each sensor's trace with a reference sensor's trace over the signal gate. The time shifts used are those giving the maximum crosscorrelation

coefficient. The diversity-stack beam is formed using the adjusted delays and diversity-stack weights, equal to the square roots of the signal power for the trace normalized by the sum of the weights for all traces.

B. SINGLE-SENSOR ANALYSIS

1. Signal Similarity

Qualitative estimates of signal similarity were made by visually comparing the unfiltered single-sensor waveforms of two Caspian Sea-Greece-Turkey events having high SNR's. Signal similarity among sensors for these events (Figures IV-1 and IV-2) was generally good over the entire trace. Visual estimates of single-sensor signal similarity for the Kamchatka events were not possible due to their low SNR's.

Using filtered data crosscorrelations were measured between sensors 1 and the remaining sensors over the signal gate; high-crosscorrelation coefficients implied good signal similarity. The average crosscorrelation coefficient for the Caspian Sea-Greece-Turkey events was 0.92 between sensor 1 and both inner and outer rings suggesting excellent signal similarity. The Kamchatka events, in general, had an extremely low average correlation coefficient of 0.42 with the exception of event NKA/311/20K which had a correlation coefficient of 0.82. For all events the deviation of individual sensor crosscorrelation coefficients from the average value was small implying consistent similarity or lack thereof among sensors.

2. Amplitude Variations

Signal amplitude variations between sensors were relatively small. For example, for the event GTU/318/15K, the filtered zero-to-peak values varied from 15.7 mμ at sensor 14 to 26.6 mμ at sensor 18 and for the event SKA/321/17K, they varied from a minimum of 5.1 mμ at sensor 19 to a maximum of 11.3 mμ at sensor 16. For the eight events the maximum single-sensor zero-to-peak value had a 22.9 mμ average, and the minimum single-sensor

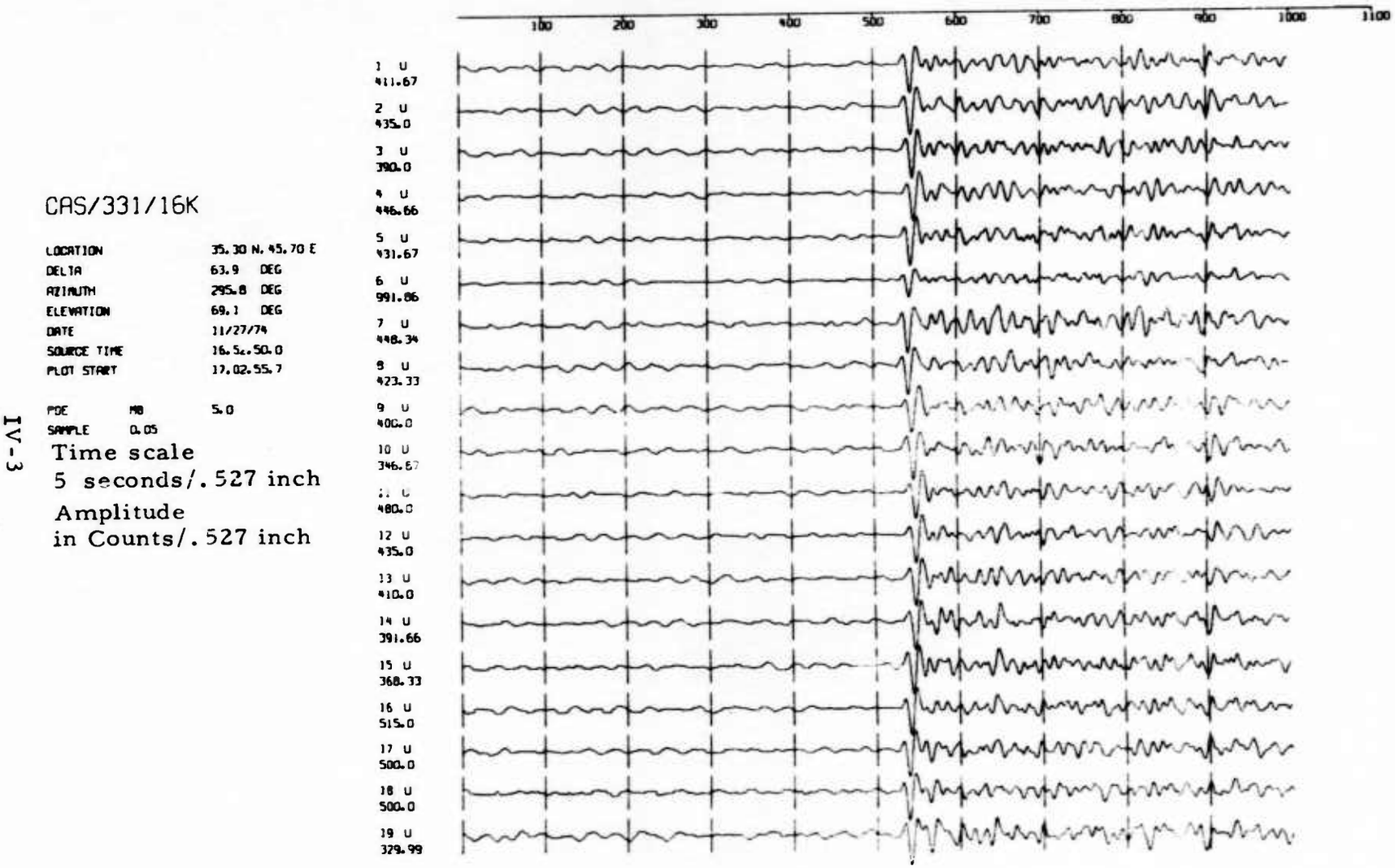

FIGURE IV-1

SINGLE-SENSOR TRACES FOR EVENT CAS/331/16K

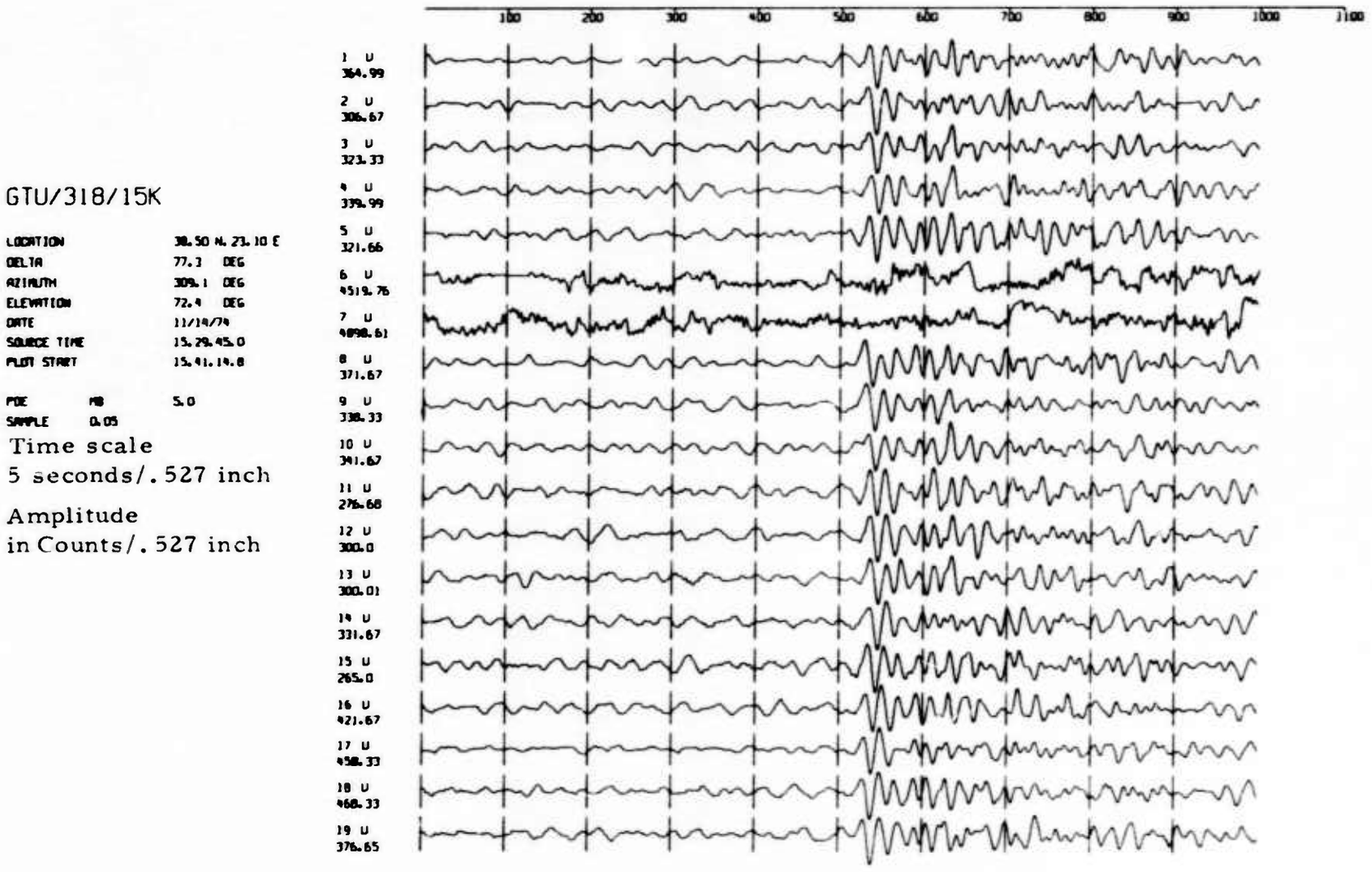

FIGURE IV-2

SINGLE-SENSOR TRACES FOR EVENT GTU/318/15K

average was 13.0 mμ. There were no consistent correlations between signal azimuth and sensors having the maximum or minimum peak values.

Table IV-1 shows the ratio (in dB) of the largest to the smallest sensor RMS signal level for all eight events. The signal calculations were made over a 6.4 second gate beginning just prior to the P-wave arrival. The events are grouped by region, and the sensors having the largest and smallest signal levels are also listed. The average of the signal amplitude variations was 1.3 dB, as compared with 3.0 dB obtained at NORSAR by Barnard and Whitelaw (1972). The variations showed no regional dependence.

C. BEAMFORMING

1. Time-Delay Anomalies

Intersensor time-delay anomalies representing deviations from plane wave propagation were calculated by computing the crosscorrelation functions between sensor 1 and the remaining sensors using filtered data. The traces were time-shifted over the signal gate until their crosscorrelation functions were maximized. The time shift at which this occurred was chosen as the adjusted delay for that event. A signal gate of 1.5 seconds was used in the computations.

Table IV-2 shows the anomalies for the Caspian Sea-Greece-Turkey events where consistent delays were obtained. Individual sensor delay anomalies between events differed by a maximum of 0.1 seconds. In general, the average delay anomaly for each event was nearly zero.

Consistent delays could not be obtained for the events from Kamchatka listed in Table IV-3 where delay anomalies varied by as much as 1.30 seconds from event to event. Two Kamchatka events had such low SNR's that the measured correlation reflected the random correlations found in noise rather than true signal similarity. This explains the inconsistencies of the delay anomalies found. The delay anomalies for this event NKA/311/20K shown in Table IV-3 were calculated by picking the correlation peak nearest to the plane wave delays, giving reasonable results. More work is needed before conclusive results can be stated about the delay anomalies for nearby events.

TABLE IV-1

MAXIMUM VARIATION OF SINGLE-SENSOR RMS CODA LEVELS ACROSS KSRS

Event	m_b	Δ^o	Azimuth (Degree)	RMS Variation max/min (dB)	Maximum Sensor	Minimum Sensor
CAS/317/02K	5.1	59.9	302.9	1.2	11	2
CAS/321/15K	5.7	59.7	290.8	1.2	16	12
CAS/331/16K	5.0	63.9	295.8	1.2	17	10
GTU/318/14K	5.1	77.3	309.2	1.2	18	15
GTU/318/15K	5.0	77.3	309.1	1.2	18	14
SKA/311/15K	4.4	24.1	47.1	1.5	8	15
NKA/311/20K	4.7	30.4	41.4	1.4	7	14
SKA/321/17K	5.0	27.2	41.2	1.5	16	19

Average variation (all events) = 1.3

TABLE IV-2

DELAY ANOMALIES FOR THE CASPIAN SEA-GREECE-TURKEY EVENTS

Sensor	Delay Anomalies (Seconds)				
	CAS/317/02K Δ = 59.9° Azimuth = 302.9	CAS/321/15K Δ = 59.7° Azimuth = 290.8	CAS/331/16K Δ = 63.9° Azimuth = 295.8	GTU/318/14K Δ = 77.3° Azimuth = 309.2	GTU/318/15K Δ = 77.3° Azimuth = 309.1
1	0.00	0.00	0.00	0.00	0.00
2	0.00	-0.05	-0.05	0.00	0.00
3	0.05	0.00	0.00	0.05	0.05
4	0.05	0.05	0.00	0.00	0.05
5	0.00	0.05	0.00	0.00	0.05
6	-	-	-0.05	-	-
7	-	0.00	-0.05	-	-
8	0.05	0.00	-0.05	0.00	0.05
9	0.05	-0.05	-0.05	0.05	0.05
10	0.00	0.00	-0.05	0.00	0.00
11	0.00	0.00	-0.05	0.05	0.10
12	-0.05	0.00	0.00	0.05	0.05
13	0.10	0.00	0.00	0.05	0.05
14	0.05	0.05	0.05	0.00	0.00
15	0.10	0.05	0.05	0.05	0.00
16	0.10	0.00	0.05	0.00	0.00
17	0.05	0.05	0.00	0.00	0.00
18	0.05	0.00	0.05	-0.05	0.00
19	0.05	-0.05	-0.05	-0.05	-0.05

TABLE IV-3

DELAY ANOMALIES FOR THE KAMCHATKA EVENTS

Sensor	Delay Anomalies (Seconds)		
	NKA/311/20K Δ = 30.4° Azimuth = 30.4	SKA/311/15K Δ = 27.2° Azimuth = 24.2	SKA/321/17K Δ = 27.2° Azimuth = 41.2
1	0.00	0.00	0.00
2	0.00	0.05	-0.10
3	0.00	0.15	0.00
4	0.00	0.50	-0.15
5	0.00	0.10	-0.15
6	0.00	-0.70	-
7	0.00	-	-0.75
8	-	-0.70	0.00
9	0.05	0.05	0.50
10	0.00	0.10	0.50
11	0.05	-0.05	-0.05
12	-0.05	-0.70	-0.05
13	0.05	-0.05	0.00
14	-0.05	-0.70	0.60
15	0.00	0.10	0.05
16	-	-	0.70
17	0.00	0.05	-0.15
18	0.00	-0.60	-0.05
19	0.00	-0.65	-0.20

2. Signal Spectral Content

Signal spectral content was studied by computing power density spectra over a 6.4-second gate beginning just prior to the P-wave arrival. The system response was not removed; however, the spectra were normalized to 1 $m\mu^2$/Hz at 1.0 Hz.

Figure IV-3 shows the average sensor and adjusted-delay beam spectra for event GTU/318/15K (SNR = 7.6). The spectra peaked at approximately 1.0 Hz and then dropped off rapidly at higher frequencies. Signal loss and noise reduction as a result of beamforming are illustrated by the difference between the average sensor trace and the adjusted-delay beam. Signal loss was quite small for frequencies between 1.0 and 2.5 Hz.

No definitive statement can be made about the spectral content as a function of region or SNR due to the insufficient number of events detected.

3. Frequency-Wavenumber (f-k) Analysis of P-Wave Signals

Maximum likelihood f-k spectra for eight events were computed at 0.63, 0.94, 1.56, 2.03, 2.50, and 2.97 Hz. Two 6.4-second segments were stacked in the computation, and 2 percent random noise was added. Figure IV-4 illustrates the results for SKA/311/15K at 0.94 Hz. The great-circle azimuth to this event was 47.1° and the Jeffreys-Bullen(J-B) tables (Richter, 1958) gave a phase velocity of 11.1 km/sec for an event at its distance. The dot on the f-k plane indicates the power density peak, suggesting that energy was propagating from 51° at 13.4 km/sec for this sample. These results are in satisfactory agreement with the predicted ones, considering the small number of segments stacked.

Table IV-4 summarizes the results of the f-k spectral analysis. In general they are consistent with propagation near the great-circle azimuth

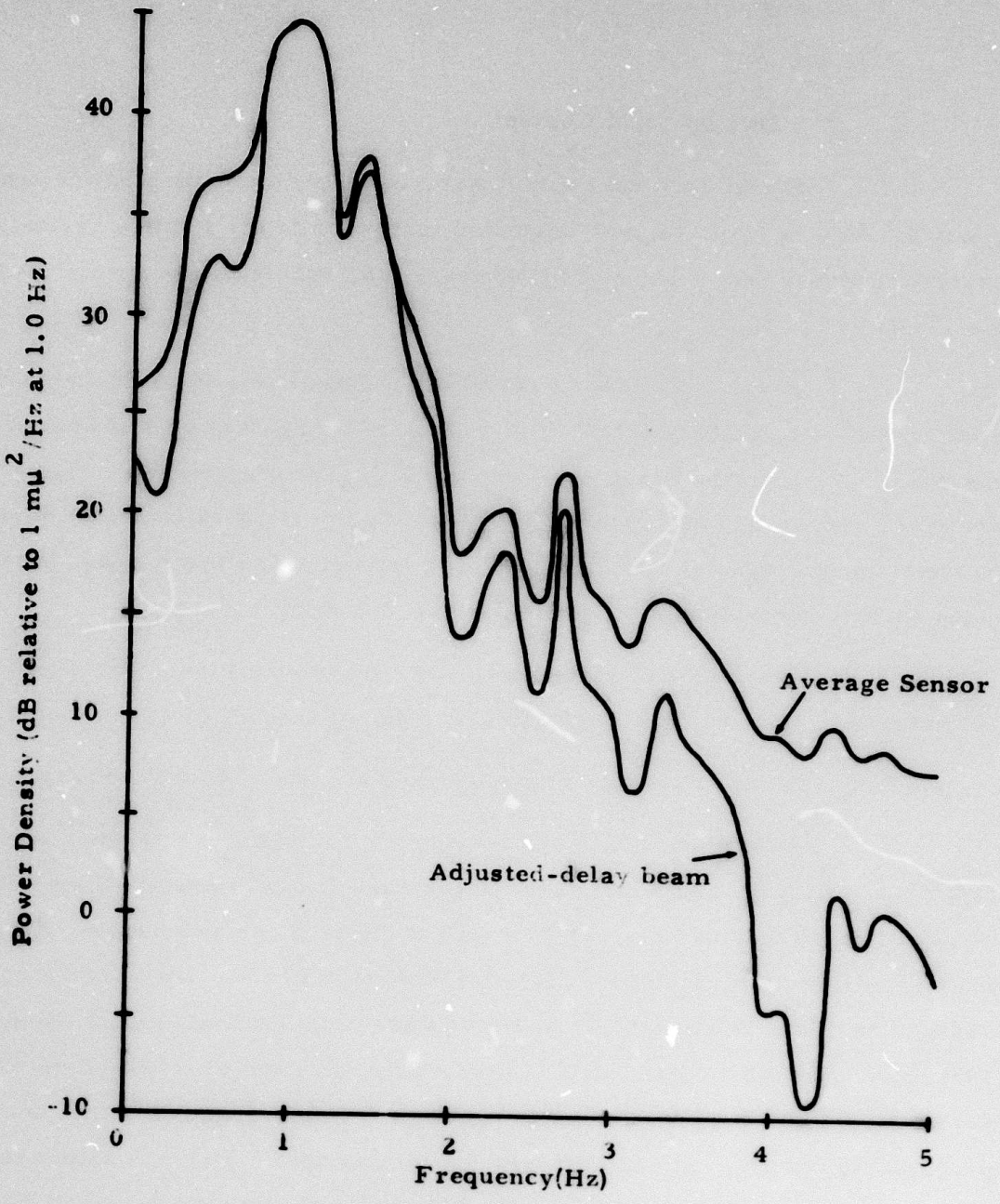

FIGURE IV-3

AVERAGE SENSOR AND ADJUSTED-DELAY BEAM SIGNAL SPECTRA OF EVENT GTU/318/1 K

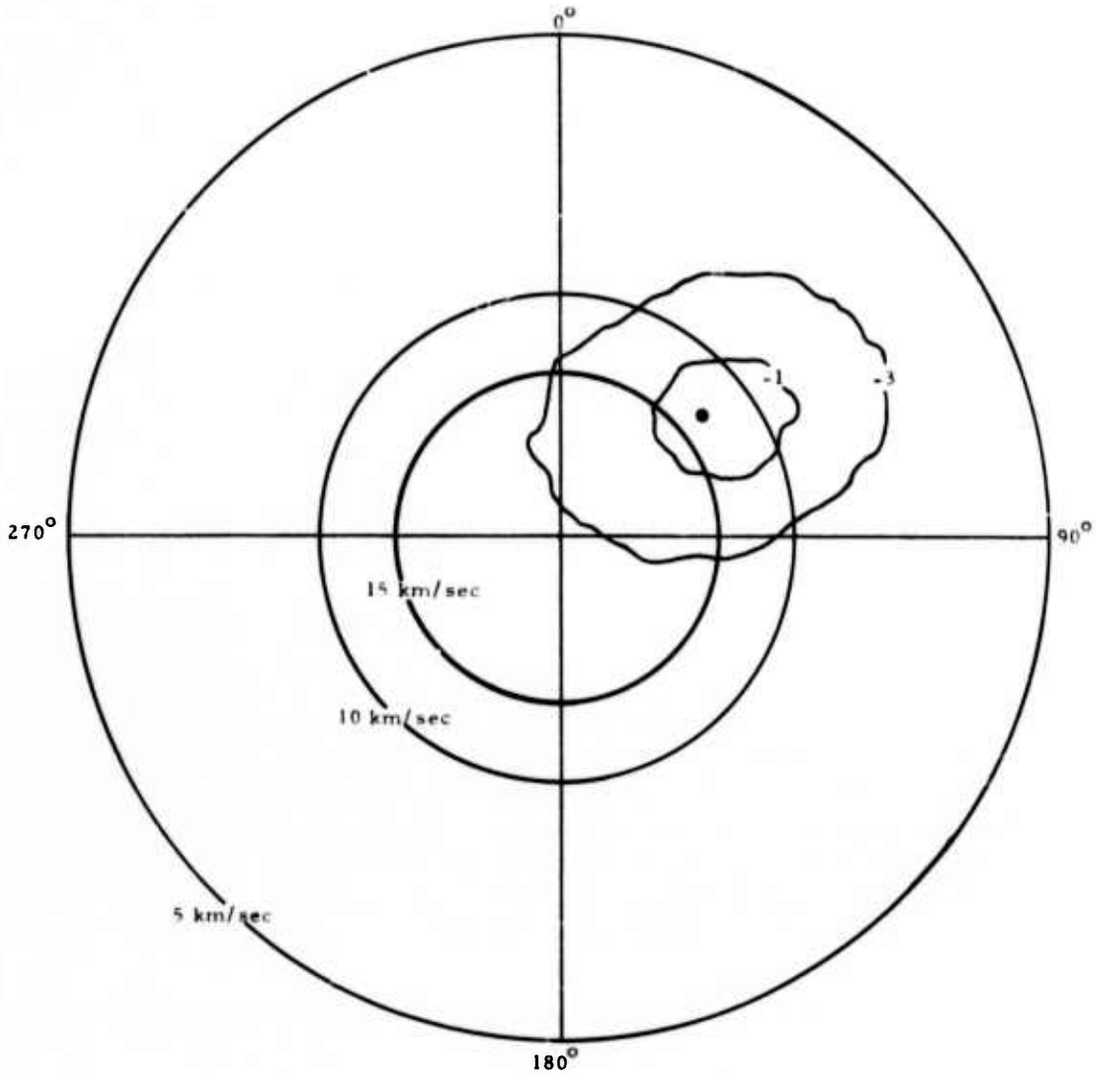

FIGURE IV-4

FREQUENCY-WAVENUMBER SPECTRUM FOR
SKA/311/15K AT 0.94 Hz

TABLE IV-4

SUMMARY OF f-k SPECTRAL ANALYSIS FOR THE EIGHT SEISMIC DATA SAMPLES
(PAGE 1 OF 2)

Event	Great-Circle Azimuth (Degrees)	J-B Velocity (km/sec)	Frequency (Hz)	Peak Power (dB)	Peak Azimuth (Degrees)	Apparent Velocity (km/sec)	-1 dB Azimuthal Range (Degrees)	Comments
SKA/311/15	47.1	11.1	0.63	17.8	-	-	-	Noise.
			0.94	17.2	51	13.4	38- 72	
			1.56	21.3	44	12.0	42- 52	
			2.03	5.0	186	18.8	158-182	Noise.
			2.50	0.9	39	13.2	37- 52	
SKA/321/17	41.2	11.5	2.03	17.5	-	-	-	Secondary peak at 36° and 12.7 km/sec. Noise at other frequencies.
NKA/311/20	41.4	12.0	0.63	21.5	-	-	-	Noise.
			0.94	21.4	32	14.0	12- 55	
			1.56	23.7	35	12.0	35- 44	
			2.03	15.8	29	13.5	25- 45	
			2.50	9.4	39	13.5	38- 47	
			2.97	7.2	35	13.1	35- 43	
CAS/317/02	302.9	17.0	0.63	30.6	312	20.1	-	
			0.94	43.7	292	18.7	282-305	
			1.56	25.3	306	14.3	283-321	
			2.03	18.5	295	14.5	282-304	
			2.50	9.0	278	5.8	275-283	
			2.97	10.7	300	14.8	290-310	

TABLE IV-4

SUMMARY OF f-k SPECTRAL ANALYSIS FOR THE EIGHT SEISMIC DATA SAMPLES
(PAGE 2 OF 2)

Event	Great-Circle Azimuth (Degrees)	J-B Velocity (km/sec)	Frequency (Hz)	Peak Power (dB)	Peak Azimuth (Degrees)	Apparent Velocity (km/sec)	-1 dB Azimuthal Range (Degrees)	Comments
CAS/321/15	290.8	17.0	0.63	37.8	256	12.5	220-292	
			0.94	35.6	285	17.0	270-305	
			1.56	30.9	284	16.6	276-286	
			2.03	28.8	282	14.5	282	
			2.50	19.9	276	13.6	275-285	
			2.97	9.2	276	14.3	276-285	
CAS/331/16	295.8	17.7	0.63	32.3	291	13.6	267-316	
			0.94	37.2	281	14.4	268-300	
			1.56	35.7	287	13.0	280-295	
			2.03	26.0	290	16.9	290	
			2.50	24.7	290	16.7	282-300	
			2.97	7.7	290	14.9	277-305	
GTU/318/14	309.2	21.0	0.63	32.3	314	14.9	275-350	
			0.94	39.9	306	23.4	300-315	
			1.56	28.1	309	31.2	290-340	
			2.03	22.3	305	21.4	297-316	
			2.50	16.8	92	5.0	-	Noise.
			2.97	7.9	315	27.0	307-330	
GTU/318/15	309.1	21.0	0.63	36.1	310	15.6	275-337	
			0.94	43.0	307	22.3	290-330	
			1.56	34.2	306	20.8	300-320	
			2.03	25.7	307	21.4	300-312	
			2.50	15.4	308	30.0	290-328	
			2.97	9.4	306	21.2	292-312	

at velocities near those predicted by the J-B tables. Variations from the predicted values suggest the presence of scattering by geological inhomogeneities or of instability in the calculations due to the small number of segments used.

4. Signal Degradation

The signal degradation is defined as the ratio of the beam power to the average single-sensor power both calculated over a 6.4 second p-wave gate. Signal degradations for both broadband and standard-filtered adjusted delay and plane wave beams are listed in Table IV-5. Broadband degradations are not given for the Kamchatka events (due to SNR's less than 1.0 dB), nor are adjusted-delay degradations given for events SKA/311/15K and SKA/321/17K due to invalid delay anomalies.

Average broadband signal degradation for the Caspian Sea-Greece-Turkey events was typically 1.6 dB for both the plane-wave and adjusted-delay beams. Average signal degradation for these beams after filtering was 1.3 dB for the plane-wave beam and 0.9 dB for the adjusted-delay beam. The Kamchatka events had average signal degradation of 1.8 dB for the filtered plane-wave beam. In general, average signal degradation for all events was 1.6 dB for broadband beams and 1.3 dB for filtered beams, and signal degradation was less for events having higher SNR's.

5. SNR Improvements Due to Beamforming

For eight events single-sensor signal powers over a 6.4-second gate starting just before the signal arrival were averaged over all operating sensors. Noise powers for the same sensors over a longer gate starting approximately 160 seconds and ending about 5 seconds before the signal arrival were also averaged. From these results an average sensor SNR was computed and compared with similarily computed SNR's for the plane-wave, adjusted-delay, and diversity-stack beams. All beams were formed using the standard

TABLE IV-5

SIGNAL DEGRADATION (in dB) FROM AVERAGE SENSOR TO PLANE-WAVE AND ADJUSTED-DELAY BEAMS

Event	Average Sensor SNR(dB)	Plane-Wave		Adjusted-Delay	
		Unfiltered	Filtered	Unfiltered	Filtered
CAS/317/02K	10.5	1.4	1.8	1.3	1.2
CAS/321/15K	14.1	3.5	1.3	3.3	1.1
CAS/331/16K	17.9	1.0	1.3	0.7	0.9
GTU/318/14K	16.0	1.9	1.2	1.8	0.9
GTU/318/15K	17.5	1.1	0.7	1.0	0.6
NKA/311/20K	9.9	-	1.4	-	1.6
SKA/311/15K	7.2	-	1.7	-	-
SKA/321/17K	5.2	-	2.3	-	-

filter. The invalid delay anomalies for the Kamchatka events (SKA/311/15K and SKA/327/17K) prevented the calculation of SNR improvements for the adjusted-delay and diversity-stack beams. Table IV-6 displays the results.

The plane-wave beam improvements averaged 11.8 dB for all eight events and showed no significant regional variations. The adjusted-delay beam improvements averaged 11.8 dB for the Caspian Sea-Greece-Turkey events and event NKA/311/20K.

The diversity-stack beams had SNR's very similar to the SNR's of the adjusted-delay beams, since diversity-stack beamforming gives significant improvements only when the signal powers of the sensors are greatly different and that was not the case here.

Without signal degradation the overall single-sensor to plane-wave beam noise reduction would have given an average improvement of 13.4 dB (average plane-wave signal degradation plus average plane-wave beam SNR improvement). This result agrees very well with the noise reduction due to beamforming of 13.1 dB obtained from the analysis in subsection III-F.

6. Comparison of KSRS m_b Estimates With NOAA and LASA m_b's

KSRS m_b values were measured for the eight events using the formula

$$m_b = \log \frac{A}{T} + B$$

where

A is the maximum peak-to-peak signal amplitude in mμ on the plane-wave beam correlated for instrument response

T is the period of the cycle with the maximum amplitude

B is the distance factor.

Values for B are shown in Table IV-7 and are the same as used at NORSAR (Barnard and Whitelaw, 1972).

TABLE IV-6

ARRAY BEAM SNR IMPROVEMENTS (dB)
RELATIVE TO AVERAGE SENSOR

Event	Average Sensor SNR(dB)	Plane-Wave	Adjusted-Delay	Diversity-Stack
CAS/317/02K	10.5	11.2	10.6	10.5
CAS/321/15K	14.1	12.1	12.5	12.1
CAS/331/16K	17.9	11.8	12.1	10.7
GTU/318/14K	16.0	12.0	12.0	11.7
GTU/318/15K	17.5	11.9	12.0	11.8
NKA/311/20K	9.9	11.6	11.4	11.1
SKA/311/15K	7.2	11.6	8.3	8.4
SKA/321/17K	5.2	11.8	8.8	8.7

TABLE IV-7

DISTANCE FACTOR (B) FOR COMPUTING KSRS m_b VALUES

Distance Degrees	B	Distance Degrees	B	Distance Degrees	B
0					
1	0.50	35	3.34	69	3.48
2	1.50	36	3.34	70	3.49
3	2.50	37	3.34	71	3.50
4	2.55	38	3.33	72	3.50
5	2.76	39	3.33	73	3.51
6	2.90	40	3.32	74	3.51
7	3.02	41	3.32	75	3.52
8	3.10	42	3.32	76	3.53
9	3.15	43	3.33	77	3.53
10	3.20	44	3.33	78	3.54
11	3.23	45	3.34	79	3.54
12	3.25	46	3.34	80	3.55
13	3.26	47	3.35	81	3.56
14	3.26	48	3.36	82	3.57
15	3.25	49	3.36	83	3.58
16	3.21	50	3.37	84	3.59
17	3.10	51	3.37	85	3.61
18	2.98	52	3.38	86	3.64
19	2.79	53	3.39	87	3.66
20	2.77	54	3.39	88	3.68
21	2.80	55	3.40	89	3.72
22	2.85	56	3.40	90	3.76
23	2.94	57	3.41	91	3.80
24	3.04	58	3.42	92	3.85
25	3.15	59	3.42	93	3.90
26	3.24	60	3.43	94	3.96
27	3.34	61	3.44	95	4.02
28	3.42	62	3.44	96	4.11
29	3.44	63	3.45	97	4.19
30	3.42	64	3.45	98	4.28
31	3.38	65	3.46	99	4.40
32	3.36	66	3.46	100	4.56
33	3.36	67	3.47	-	-
34	3.35	68	3.48	-	-

Figure IV-5 is a plot of KSRS m_b's versus NOAA m_b's (circles) or LASA m_b's(squares). The KSRS m_b's are generally somewhat smaller than the LASA and NOAA m_b's. This negative bias of approximately 0.3 magnitude units may be attributable to atypical local geologic structures or to incorrect B values. More data are necessary before this discrepancy can be fully explained and any regional dependencies can be found.

D. CONCLUSIONS

Signal similarity was good for the Caspian Sea-Greece-Turkey events but not for the Kamchatka events. RMS coda amplitude variations averaged 1.3 dB between sensors from event to event. Time-delay anomalies for the Caspian Sea-Greece-Turkey events were consistent and essentially zero; The cross-correlation coefficients for the Kamchatka events were often very low resulting in questionable delay adjustements of as much as 1.3 seconds. Spectra for the eight events were very similar to typical spectra at NORSAR with dominant spectral peaks occurring below 1.5 Hz. Frequency-wavenumber spectra were consistent with propagation near the great-circle azimuth at velocities near those predicted by the J-B tables. Average broadband signal degradation for the Caspian Sea-Greece-Turkey events was 1.6 dB for both the plane-wave and adjusted-delay beams while average degradation after filtering was 1.3 dB for the plane-wave beam and 0.9 dB for the adjusted-delay beam. The Kamchatka events had an average filtered signal degradation of 1.8 dB for the plane-wave beam. SNR improvements averaged 11.8 dB for the plane-wave beam. In general, adjusted-delay and diversity-stack beamforming yielded no significant SNR improvements over plane-wave beamforming.

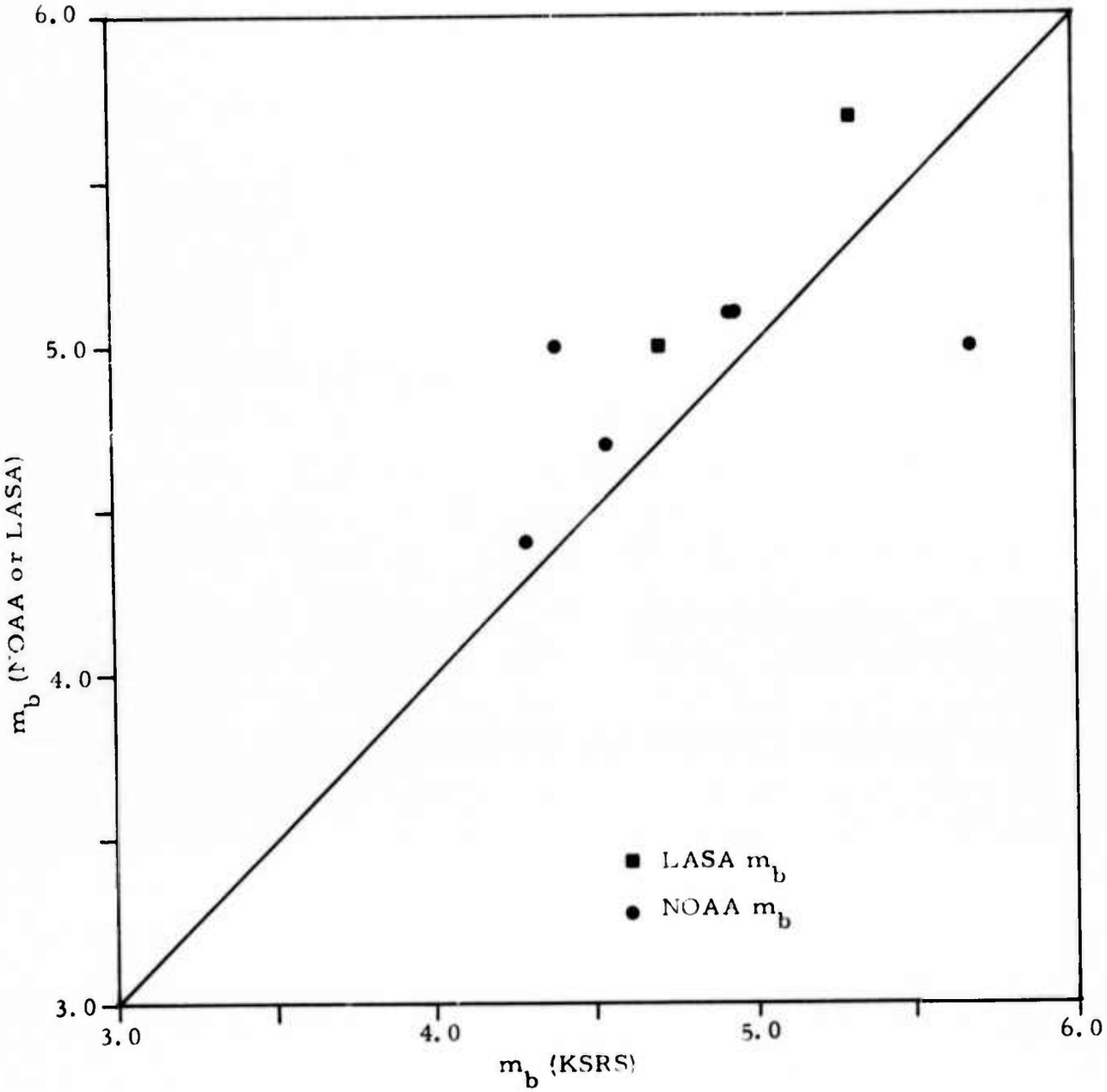

FIGURE IV-5

KSRS MAGNITUDE VERSUS NOAA OR LASA MAGNITUDE

SECTION V

PRELIMINARY ESTIMATION OF THE KSRS SP DETECTION THRESHOLD

This section presents a preliminary estimate of the KSRS SP array detection threshold. The method used was a maximum likelihood procedure that estimated the array detection threshold by comparison with an independent reference. The basic assumptions in the procedure are that the detection curve belongs to some general class of Gaussian functions and the selection of the reference events is entirely random (Ringdal, 1974). The general procedure in estimating the detection curve is as follows:

- Obtain a reference set of randomly selected events of various magnitudes
- Make a decision as to whether or not the events were detected
- Maximize the likelihood function for the observed pattern of detections and nondetections to find the values of the detection curve.

From the ensemble of 36 available events, ten events were detected by automatic procedures and ten by visual means. The histogram of the events detected or not detected versus magnitude and the maximum likelihood detectability curve are shown in Figure V-1. The 50 percent threshold estimate was 4.39 ± 0.10 magnitude units while the 90 percent threshold estimate equaled 4.90 ± 0.18. Caution must be used in evaluating the confidence limits for these estimates. The maximum likelihood estimation procedure is sensitive to bad data points and to small distributions that are not Gaussian, and a statistical population of 36 events is probably inadequate for reliable conclusions.

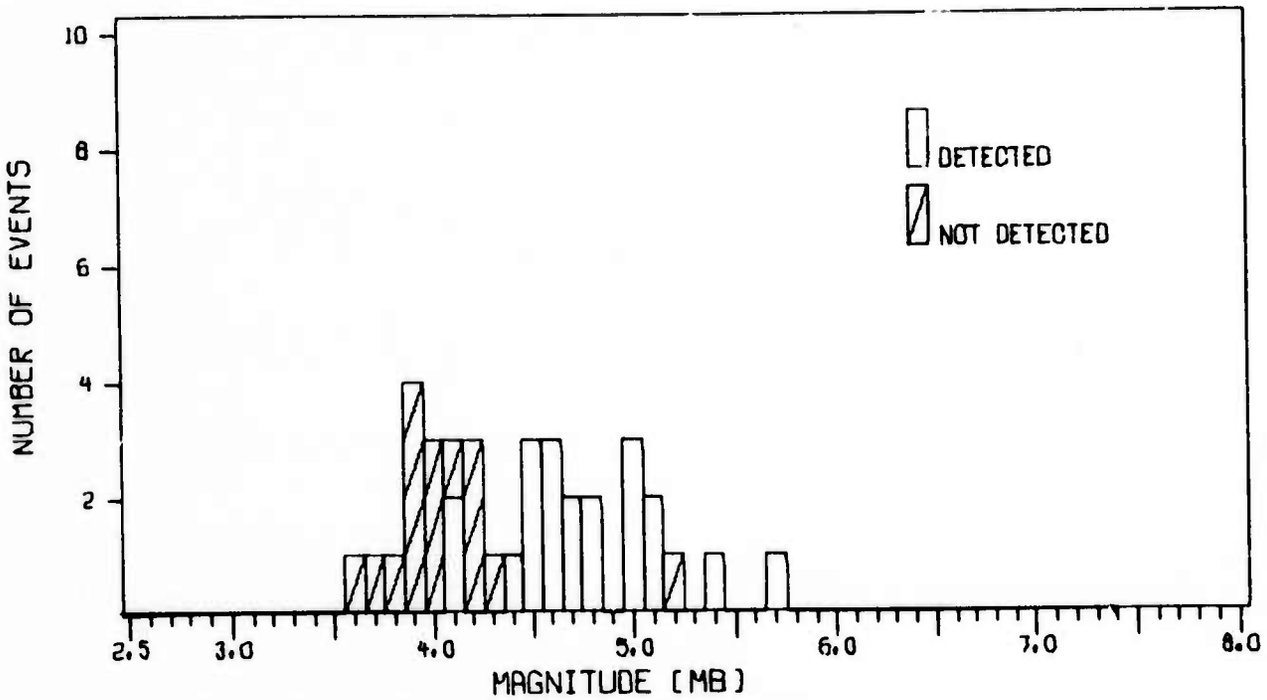

MB DISTRIBUTION OF PROCESSED EVENTS
KSRS DETECTION THRESHOLD ESTIMATION

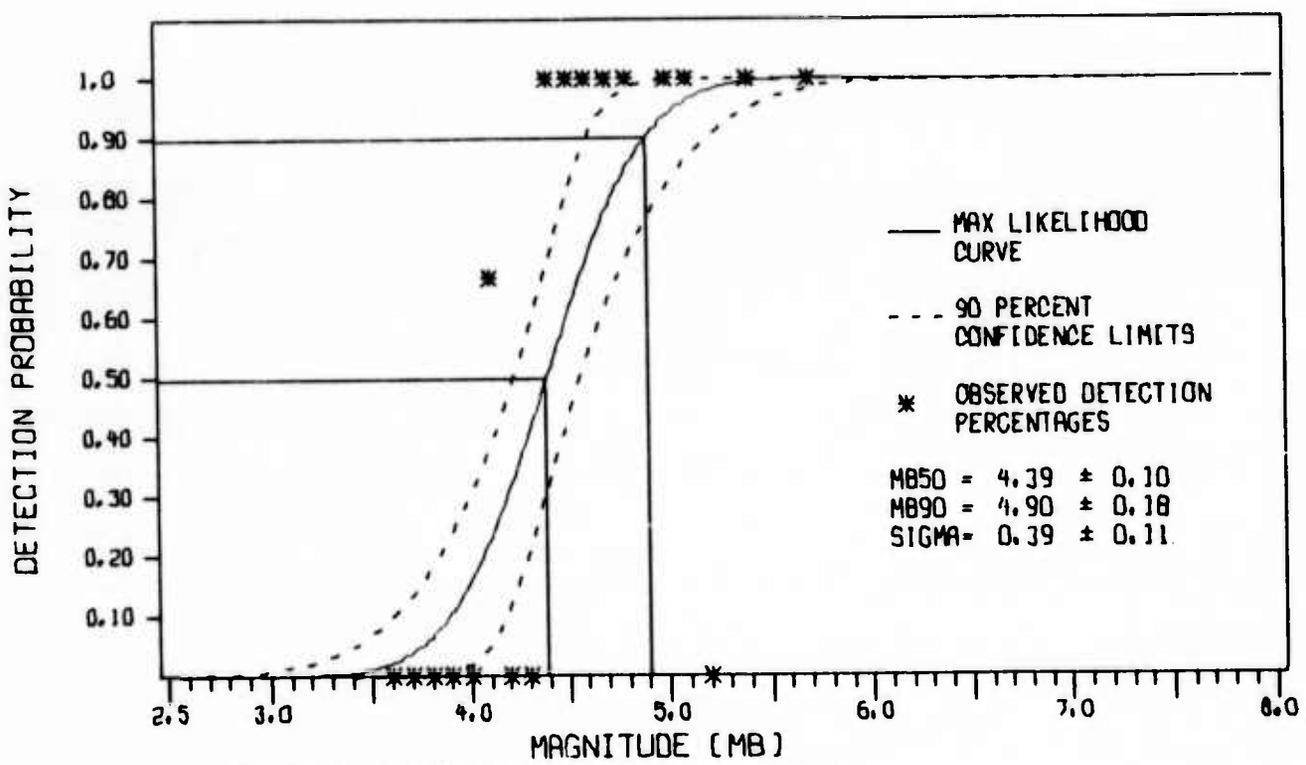

MAXIMUM LIKELIHOOD DETECTABILITY CURVE
KSRS DETECTION THRESHOLD ESTIMATION

FIGURE V-1

KSRS DETECTION THRESHOLD ESTIMATION

SECTION VI

SUMMARY AND CONCLUSIONS

Results and conclusions concerning the performance of the KSRS SP array are presented below.

KSRS had useable data for only 36 teleseismic events from a data base of 123 Eurasian events recorded during 29 April 1973 to 26 July 1973 and November 1974. Eight seismic events, five from the Caspian Sea-Greece-Turkey region and three from the Kamchatka region, had SNR greater than 5.0 (dB) and were used in the signal analyses. Nineteen useable noise samples were obtained from the November 1974 data; six of these noise samples were analyzed for this report. Data quality of the useable signal and noise samples was very good. Sensors 5, 7, 10, 16, and 17 were responsible for the majority of the data losses; however, on the average, 17 sensors were operational. There were essentially no spikes or clipped peaks in the data.

Major results and conclusions are:

1. Data Base

   - The November data was significantly superior in quality to the data from 29 April 1973 to 26 July 1973.

2. Noise Analysis

   - The noise spectra both with and without correction for instrument response were very simple with major peaks occurring in the 6-second microseismic band and rapidly decreasing amplitudes at shorter periods. A minor peak (30 dB lower than the peak at 0.16 Hz) occurred at 3.2 Hz;

this peak was not found in the NORSAR noise spectra. No significant temporal or spatial variations in the noise spectra were observed.

- Single-sensor RMS noise amplitudes averaged were 10.9 mμ for unfiltered data and 1.6 mμ for filtered data. This is approximately three times higher than the corresponding amplitudes at NORSAR.

- Multiple coherence levels were relatively low at all frequencies above 0.5 Hz. For effective calculations of SNR's, elimination of low frequency energy is essential.

- Frequency-wavenumber spectral analysis suggested that noise energy below 1 Hz was caused by Rayleigh-mode surface waves from the southwest and northeast while noise energy above 1 Hz was random.

- Noise reduction achieved by beamforming was slightly higher than theoretical random noise reduction due to the excellent suppression of the dominant propagating surface-wave energy found at low frequencies.

3. Signal Analysis

- Signal similarity, observed visually and calculated from crosscorrelation techniques, was quite good for the Caspian Sea-Greece-Turkey events. The Kamchatka events generally had poor signal similarity.

- Signal amplitude variations between sensors were relatively small with an average variation of 1.3 dB. Peak-to-peak variation at single sensors averaged 4.9 dB for all events.

- Time-delay anomalies were consistent and nearly zero for the Caspian Sea-Greece-Turkey events. The nearby Kamchatka events had inconsistent and invalid delay anomalies caused by low SNR's.

- Eurasian signals usually had similar spectral shapes and substantial amounts of high frequency (to approximately 2 Hz) energy. In general, KSRS spectra were very similar to spectra measured at NORSAR. The limited ensemble of events prevented any determination of regional dependence.

- The frequency-wavenumber spectral analyses were consistent with propagation near the great-circle azimuth at velocities near those predicted by the Jeffreys-Bullen tables.

- Array beamforming signal degradation for all events averaged 1.6 dB for the filtered plane-wave beam. The average degradation for the adjusted-delay beam was 1.3 dB for the events having consistent delay anomalies. Signal degradation was less for events having higher SNR's.

- The plane-wave beam improvements in SNR averaged 11.8 dB for all events and had no significant regional variations. The adjusted-delay beam improvements averaged 11.8 dB. These values after correction for signal degradation were almost equal to the theoretical SNR improvement, 10 log (number of sensors = 17), or 12.3 dB. In general, no significant SNR improvements were obtained by adjusted-delay and diversity-stack beamforming over plane-wave beamforming.

- KSRS m_b's averaged about 0.3 magnitude units less than LASA and NOAA m_b's. This negative bias may be attributable to atypical local geologic structures or to incorrect B values.

- For detection of Eurasian events, a bandpass filter with approximate corner frequencies at 1.0 and 2.5 Hz and a very sharp rolloff at low frequencies appears to be optimum.

4. KSRS Detection Threshold

- A maximum likelihood procedure was used to estimate the KSRS detection threshold from a data base of 36 teleseismic events. The 50 percent threshold estimate was 4.39 ± 0.10 magnitude units while the 90 percent threshold estimate was $m_b = 4.90 \pm 0.18$. These results are probably unreliable due to the small data sample used.

SECTION VII
REFERENCES

Barnard, Thomas E., and Richard L. Whitelaw, 1972, Preliminary Evaluation of the Norwegian Short Period Array, Special Report No. 6, AFTAC Contract Number F33657-71-C-0843, Texas Instruments Incorporated, Dallas, Texas.

Haubrich, R. A., and K. McCamy; 1969, Microseisms: Coastal and Pelagic Sources, Review of Geophysics, 7, p. 539.

Richter, Charles F., 1958, Elementary Seismology, W. H. Freeman and Co., Inc., San Francisco, California.

Ringdal, Frode, and Richard L. Whitelaw, 1973, Evaluation of the Norwegian Short-Period Array-Final Report, Special Report No. 11, Texas Instruments Report No. ALEX(01)-STR-73-11, Contract Number F33657-72-C-0725, Texas Instruments Incorporated, Dallas, Texas.

Ringdal, Frode, 1974, Estimation of Seismic Detection Thresholds, Technical Report No. 2, Texas Instruments Report No. ALEX(01)-TR-74-02, Contract Number F08606-74-C-0033, Texas Instruments Incorporated, Dallas, Texas.

Texas Instruments Incorporated, 1971, Documentation of Off-Line Array Evaluation Software Package, Long Period Array Processing Development, AFTAC Contract Number F33657-69-C-1063, Texas Instruments Incorporated.